EXCALIBUR : Relativistic raytracing for weak & strong lensing analysis

Laurent Magri-Stella[1,2], Narei Lorenzo Martinez[2,3], Vincent Reverdy[2,3]

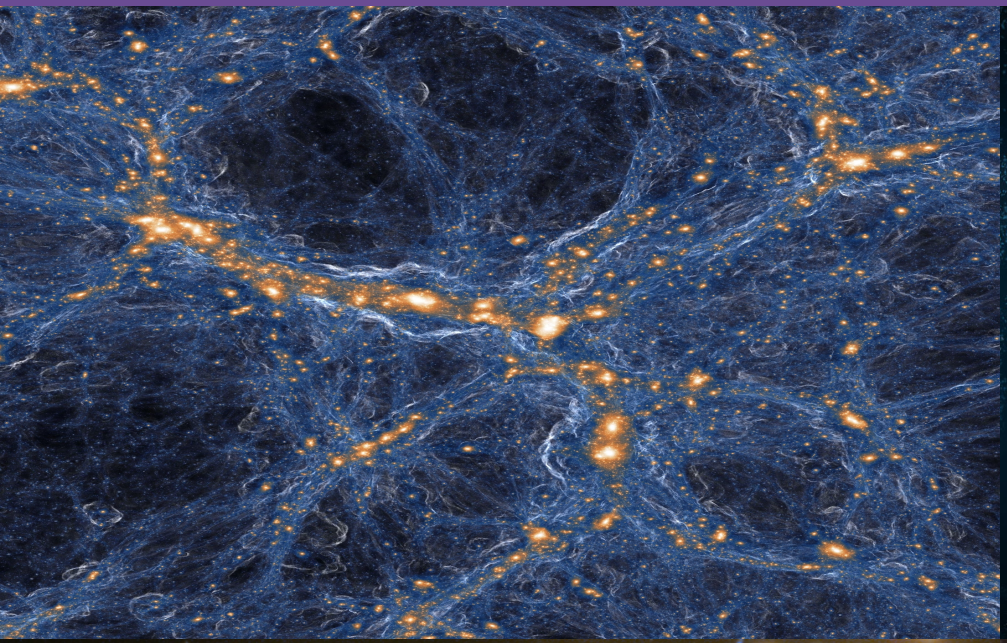
[1] Université Savoie Mont Blanc
[2] Laboratoire d'Annecy de Physique des Particules (LAPP), CNRS
9 Chemin de Bellevue, 74940 Annecy-le-Vieux
[3] Centre National de la Recherche Scientifique (CNRS)

04.11.2026





Galaxy clusters as a key cosmological probe









The upcoming surveys



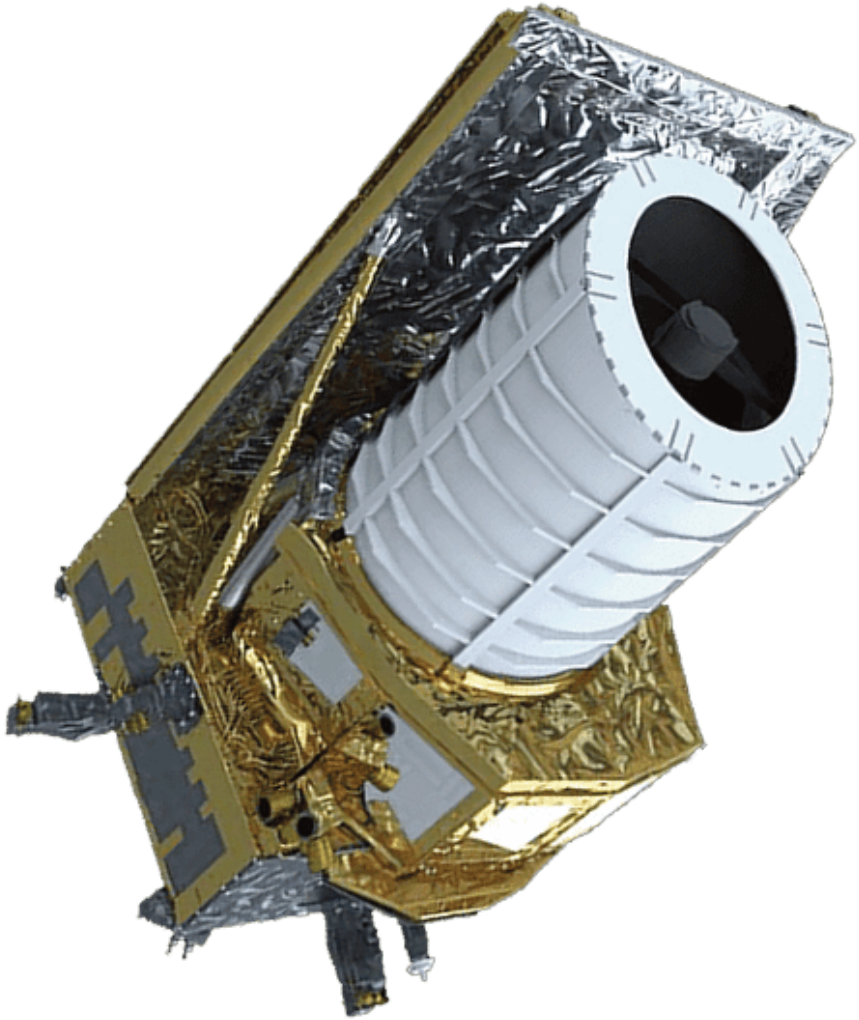
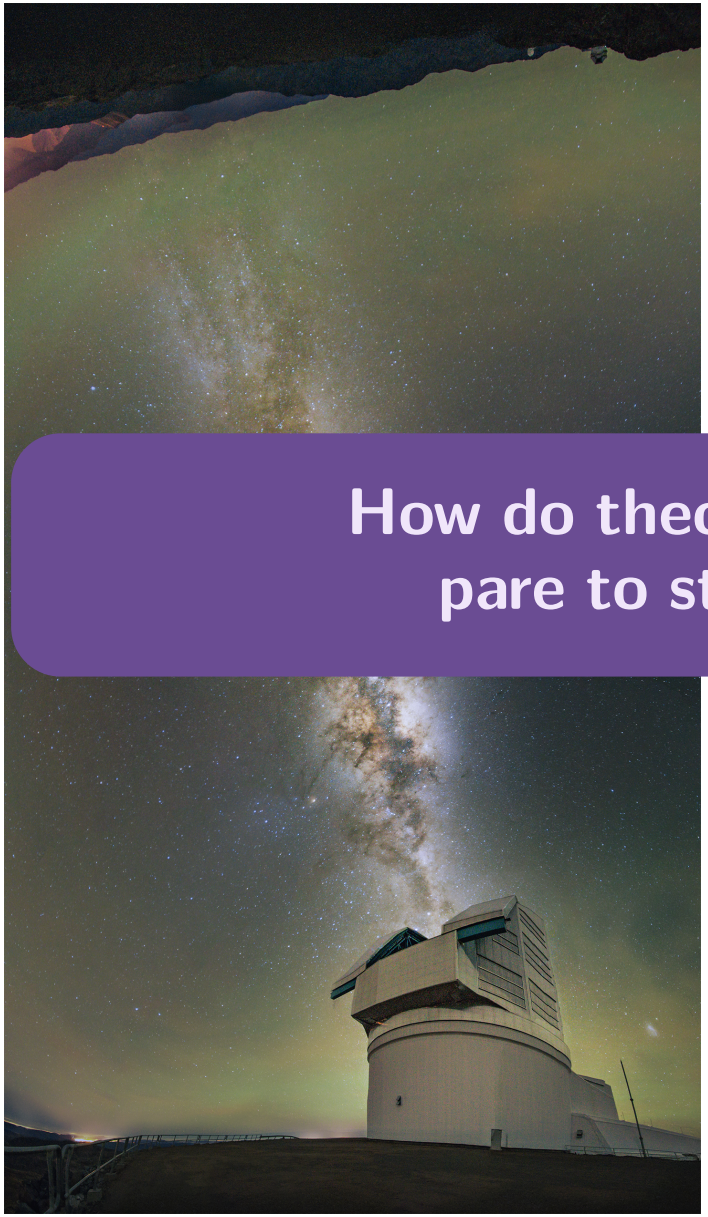


Figure 1: Vera C. Rubin Observatory (LSST) and Euclid satellite.

An important question





How do theoretical uncertainties compare to statistical uncertainties?

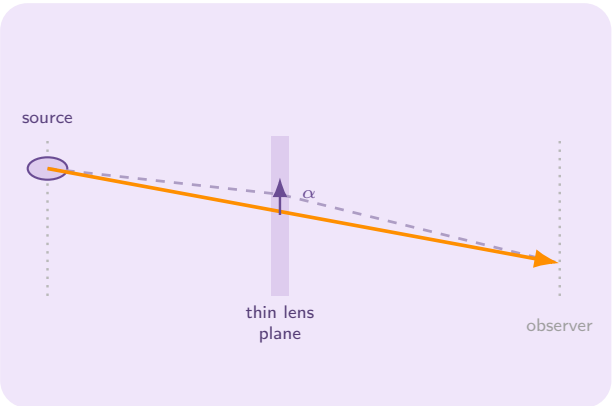
Figure 2: Vera C. Rubin Observatory (LSST) and Euclid satellite.

Towards an answer ?

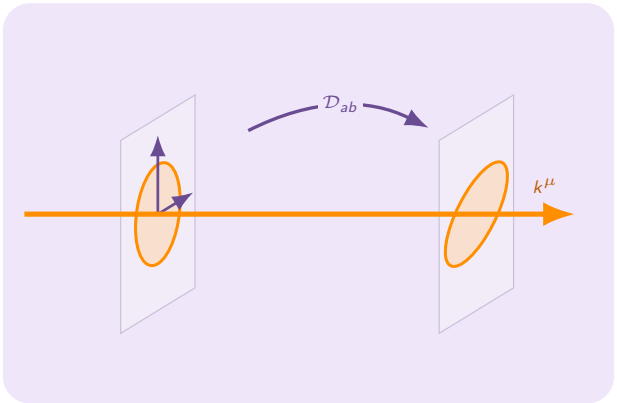
1 **Weak lensing**

2 **Sachs formalism**

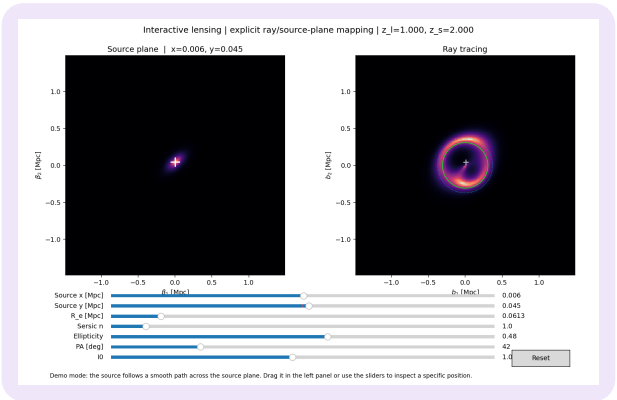
3 **EXCALIBUR**



Current weak-lensing practice and its main approximations.



Relativistic beam propagation and distortions from curvature.



Relativistic raytracing for weak & strong lensing in FLRW space-time.

Weak lensing: a brief overview

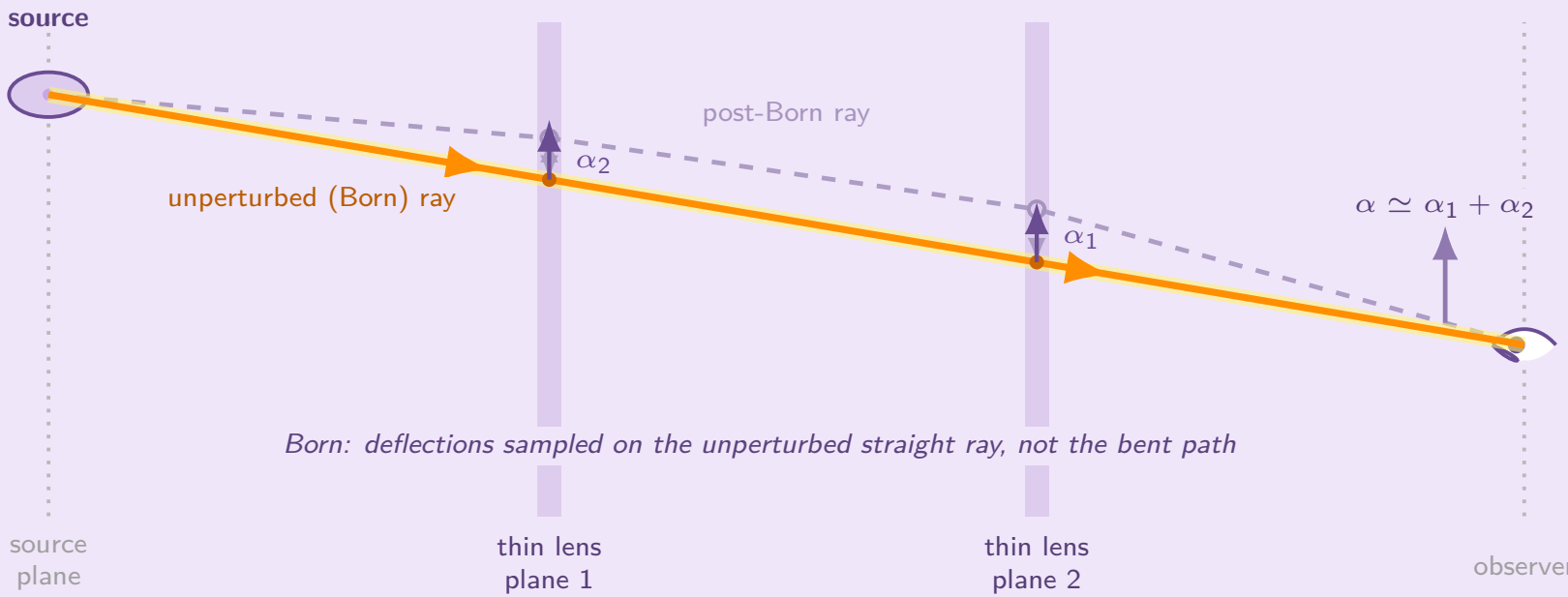


Figure 3: Current approximations in weak lensing frameworks: 1/ Born approximation 2/ thin lens planes. The dashed ray represents the post Born approach, which starts to be more commonly used in simulations, has yet to be implemented in analysis pipelines.

Lens equation and magnification matrix

$$\boldsymbol{\beta} = \boldsymbol{\theta} - \boldsymbol{\alpha}(\boldsymbol{\theta}) \qquad \frac{\partial \beta_i}{\partial \theta_j} \approx \delta_{ij} - \frac{\partial \alpha_i}{\partial \theta_j} = A_{ij}$$

Weak lensing: convergence, shear, and flexion

First order approximation of the magnification matrix

$$A = \begin{pmatrix} 1-\kappa & 0 \\ 0 & 1-\kappa \end{pmatrix} - \gamma \begin{pmatrix} \cos(2\phi) & \sin(2\phi) \\ \sin(2\phi) & -\cos(2\phi) \end{pmatrix}$$

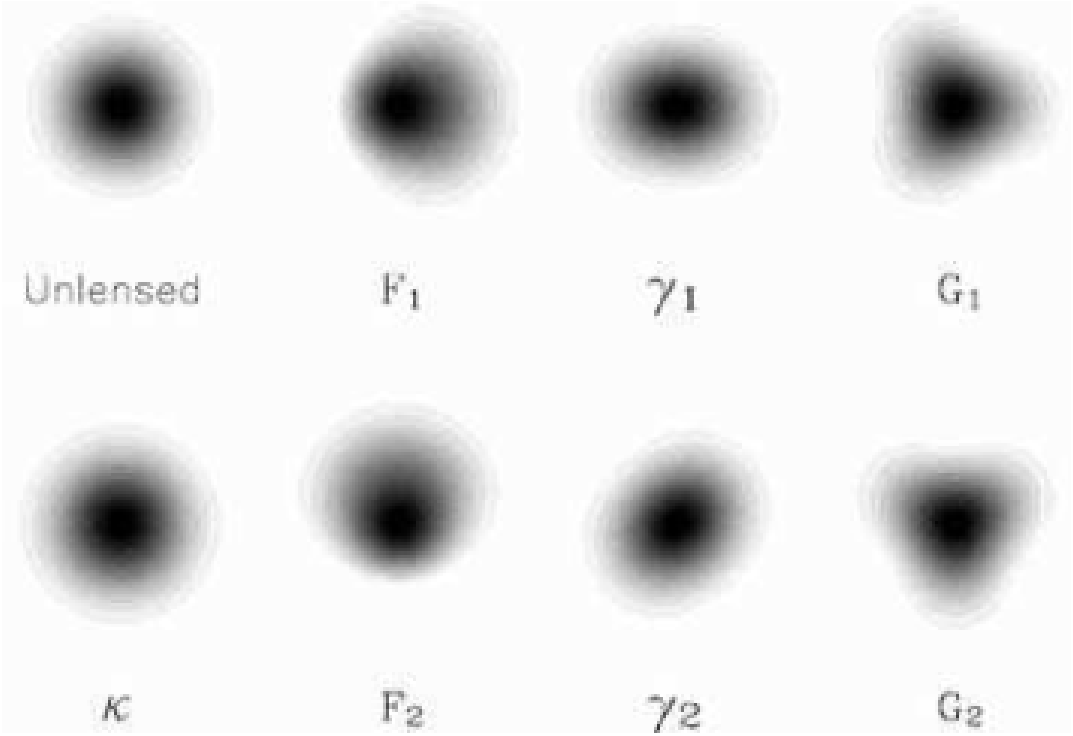


Figure 4: Effects of the different lensing fields on a Gaussian galaxy of radius 1 arcsec. 10% convergence/shear and 0.28 arcsec^{-1} flexion (which is a very high value for this quantity, chosen only to visualize) are applied. From Bacon et al. 2006

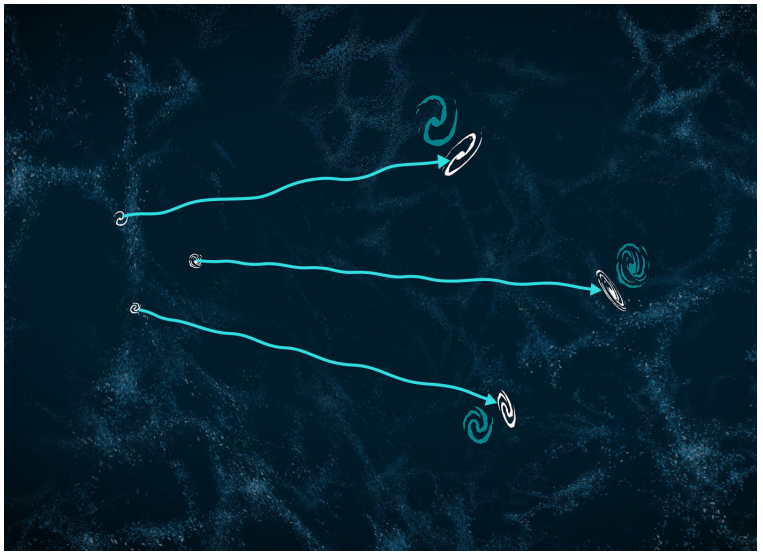
A relativistic description of light propagation

Goal

Describe light propagation directly in space-time, beyond the standard weak-lensing approximations.

Three ingredients

1. a background metric describing the geometry;
2. the geodesic equation for photon trajectories;
3. the Sachs formalism for beam deformations.



Why this drops the approximations

- Born $\rightarrow$ geodesic integrated along the true light path.
- Thin lens $\rightarrow$ continuous fields sampled in 4D.

1/ A background metric describing the geometry

The Friedmann-Lemaitre-Robertson-Walker metric

$$g_{\mu\nu} = \begin{pmatrix} -c^2 & 0 & 0 & 0 \\ 0 & \frac{a^2(t)}{1-kr^2} & 0 & 0 \\ 0 & 0 & a^2(t)r^2 & 0 \\ 0 & 0 & 0 & a^2(t)r^2\sin^2\theta \end{pmatrix}$$

where:

- $a(t)$: scale factor
- k: curvature parameter ($k = 0, +1, -1$)

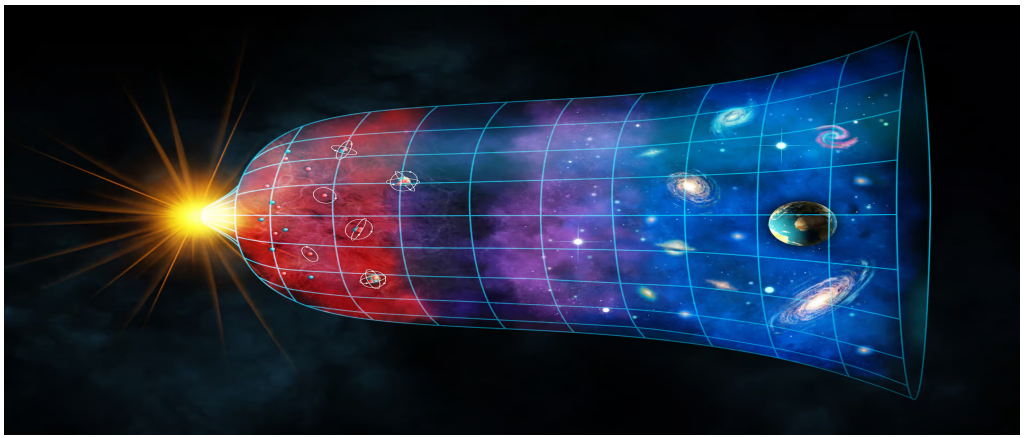


Figure 5: The story of the Universe: from the Big Bang to the present day.
Credit: Natalie Mayer

1/ A perturbed background metric describing the geometry

The perturbed Friedmann-Lemaitre-Robertson-Walker metric

$$g_{\mu\nu} = \begin{pmatrix} -c^2(1+2\Phi) & 0 & 0 & 0 \\ 0 & a^2(t)(1-2\Psi) & 0 & 0 \\ 0 & 0 & a^2(t)(1-2\Psi) & 0 \\ 0 & 0 & 0 & a^2(t)(1-2\Psi) \end{pmatrix}$$

in

- cartesian coordinates;
- flat space ($k = 0$).

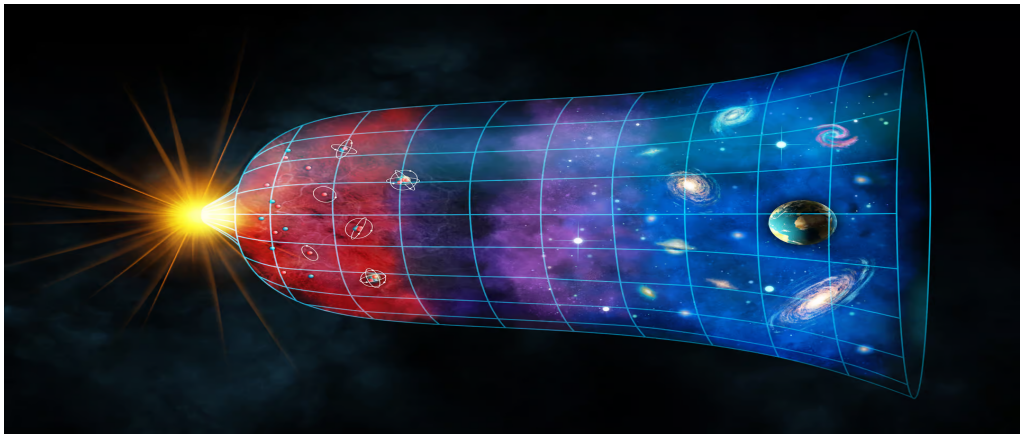
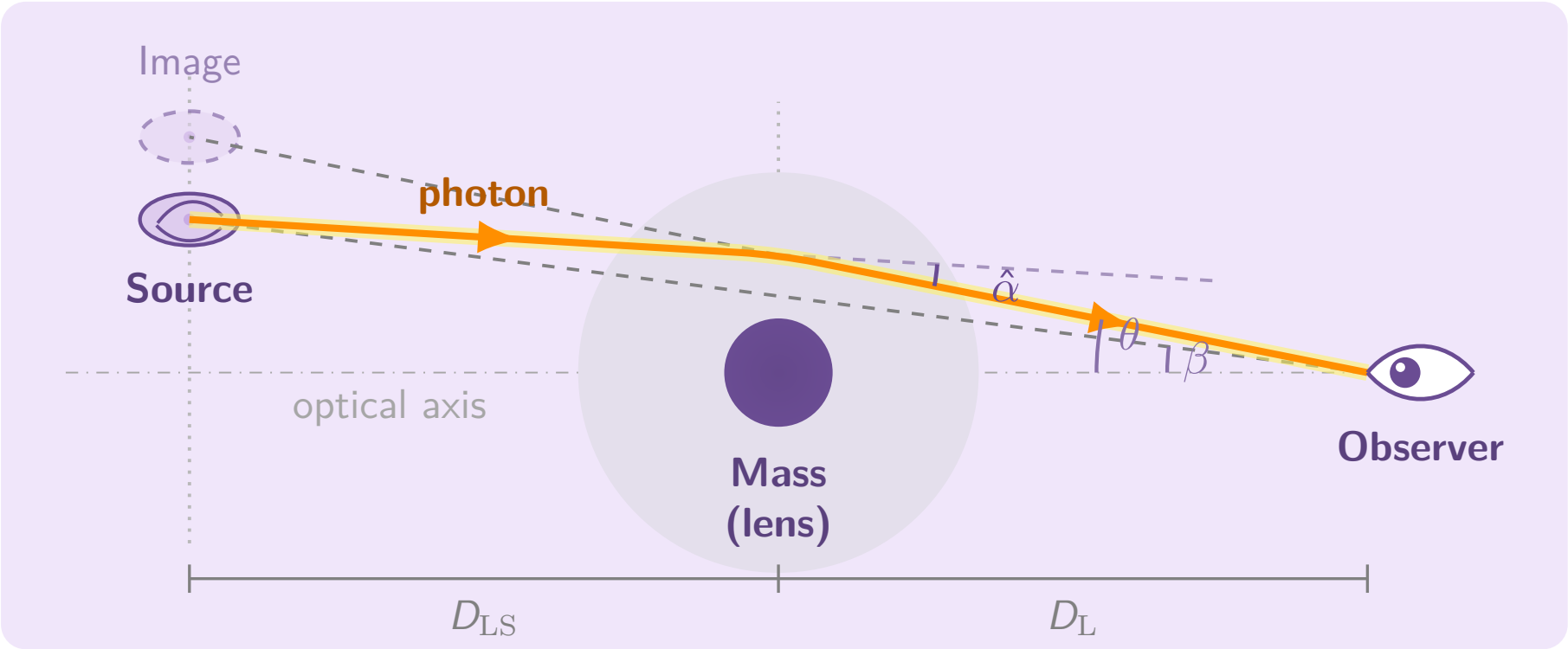


Figure 6: The story of the Universe: from the Big Bang to the present day.
Credit: Natalie Mayer

2/ The geodesic equation for photon trajectories

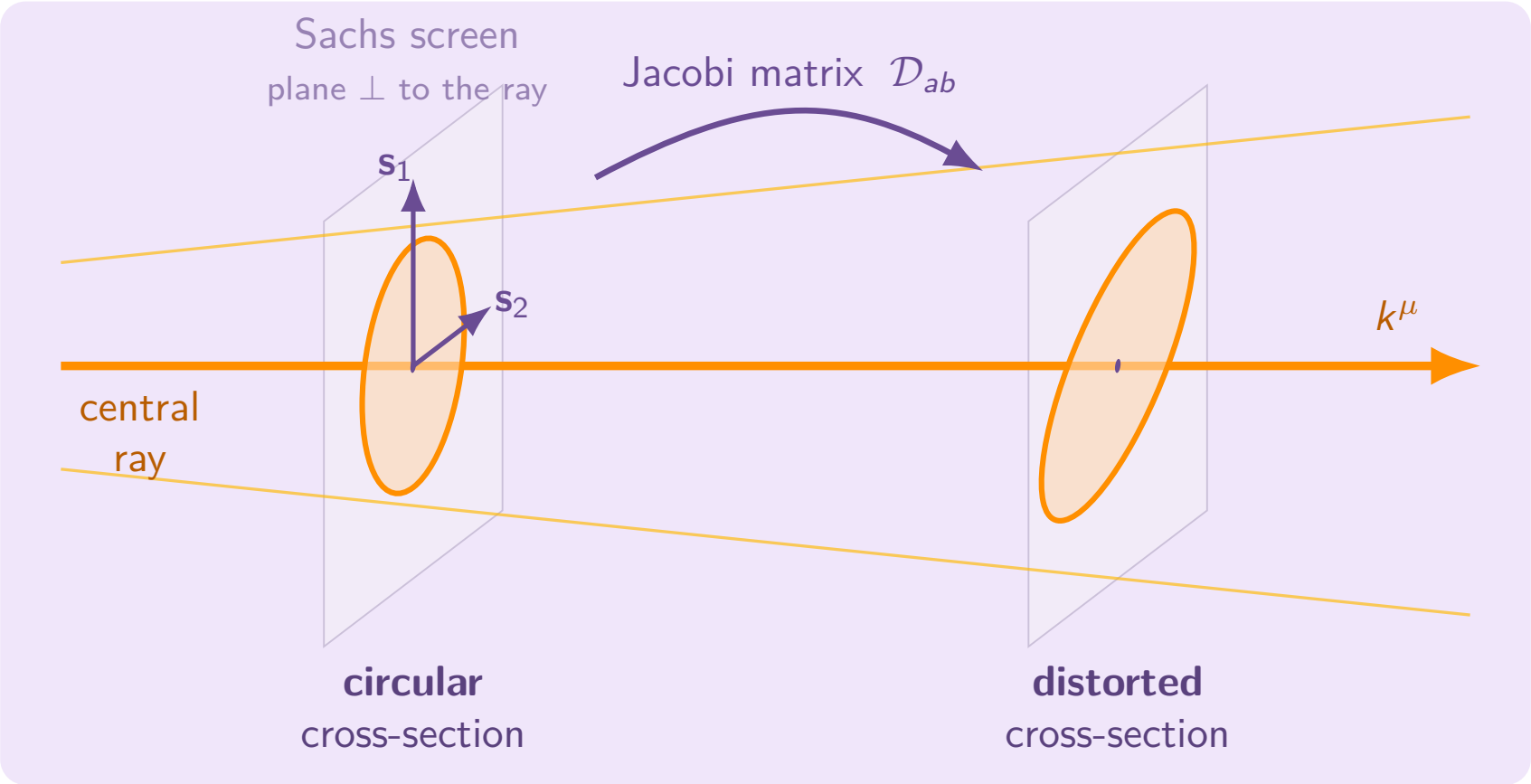


Geodesic equation

$$\frac{\mathrm{d}^2 x^\mu}{\mathrm{d}\lambda^2} + \Gamma^\mu_{\alpha\beta} \frac{\mathrm{d}x^\alpha}{\mathrm{d}\lambda} \frac{\mathrm{d}x^\beta}{\mathrm{d}\lambda} = 0 \qquad g_{\mu\nu} k^\mu k^\nu = 0$$

The metric fixes the Christoffel symbols, which determine how photon trajectories curve through inhomogeneous matter distributions.

3/ The Sachs formalism for beam deformations



Optical tidal matrix

$$\mathcal{R}_{AB} = R_{\mu\nu\rho\sigma} k^\mu s_A^\nu s_B^\rho k^\sigma$$

$$\mathcal{R}_{AB} = -\frac{1}{2} R_{\mu\nu} k^\mu k^\nu \delta_{AB} + C_{\mu\nu\rho\sigma} s_A^\mu k^\nu k^\rho s_B^\sigma$$

Focusing equation and A_{ij}

$$\frac{\mathrm{d}^2 \mathcal{D}_{AB}}{\mathrm{d}v^2} = \mathcal{R}_{AC}\, \mathcal{D}_{CB}$$

$$\mathcal{D} = A\bar{\mathcal{D}} + \dots$$

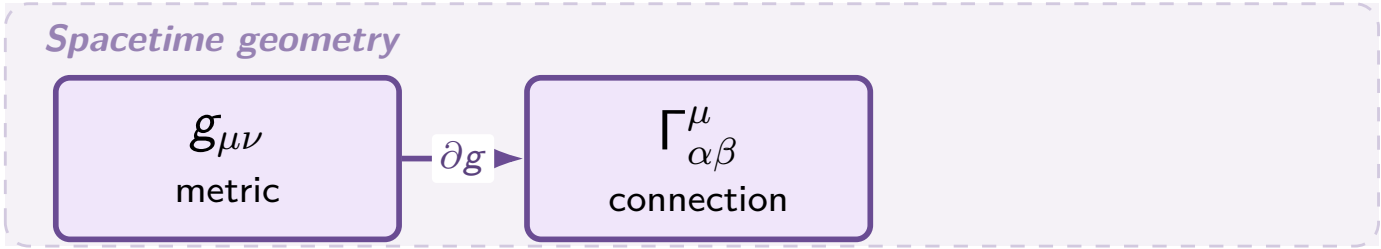
The tensor chain: from the metric to the Jacobi matrix

Spacetime geometry

$g_{\mu\nu}$
metric

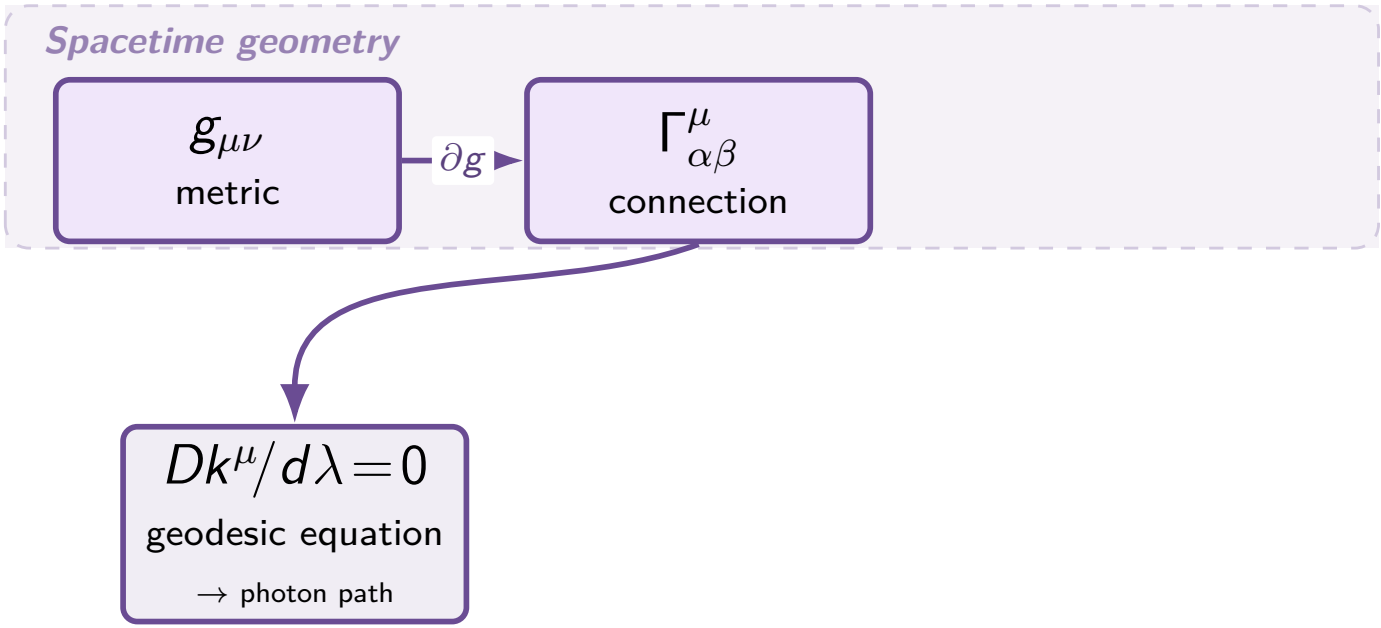
The **metric alone** fixes the whole chain: each tensor follows from derivatives of the previous one.

The tensor chain: from the metric to the Jacobi matrix



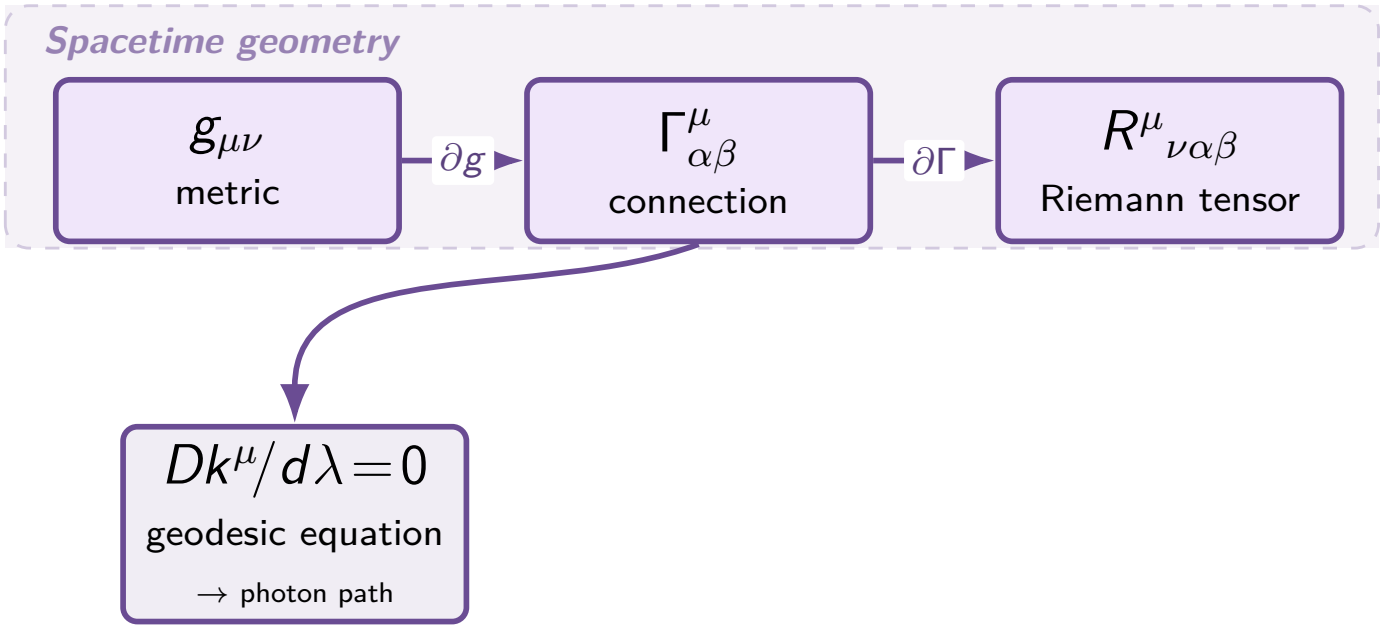
The **metric alone** fixes the whole chain: each tensor follows from derivatives of the previous one.

The tensor chain: from the metric to the Jacobi matrix



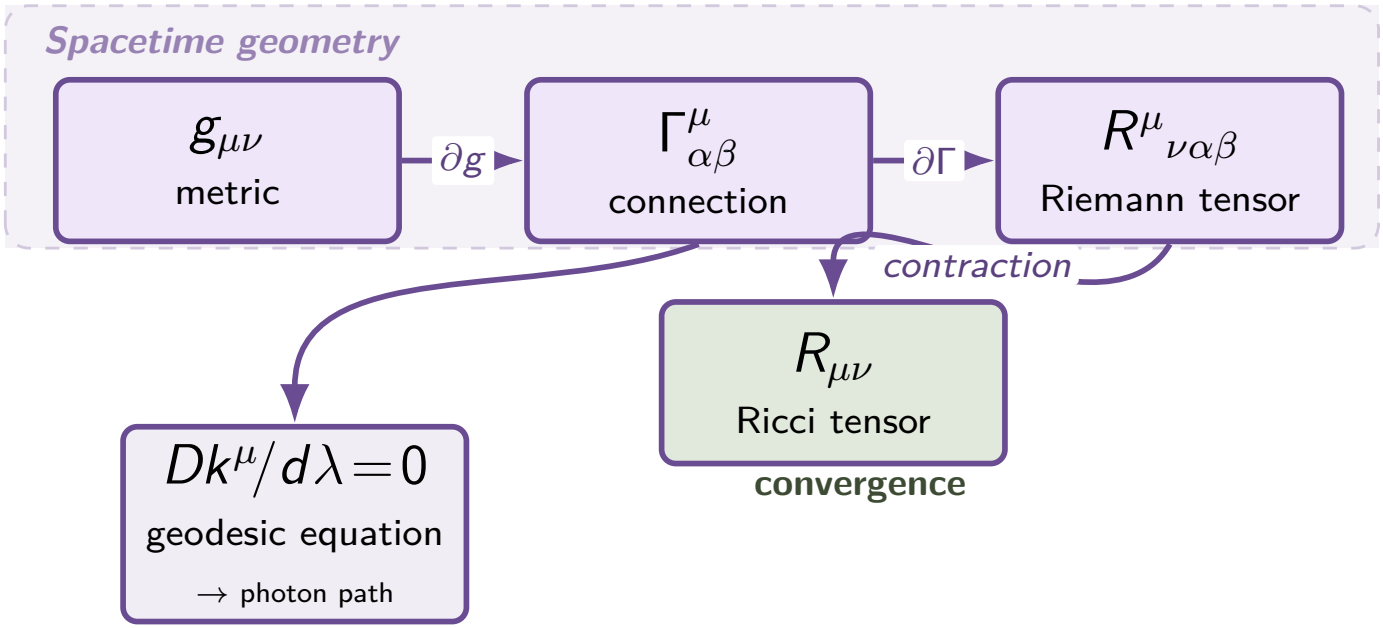
The **metric alone** fixes the whole chain: each tensor follows from derivatives of the previous one.

The tensor chain: from the metric to the Jacobi matrix



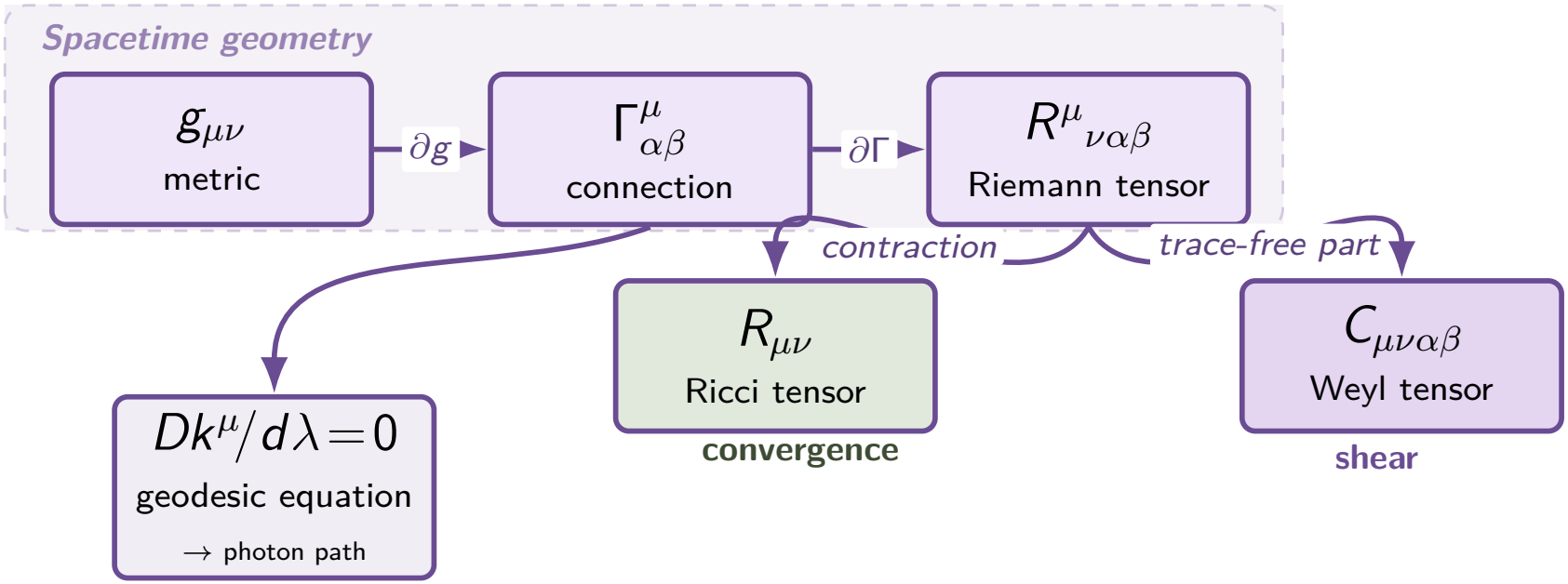
The **metric alone** fixes the whole chain: each tensor follows from derivatives of the previous one.

The tensor chain: from the metric to the Jacobi matrix



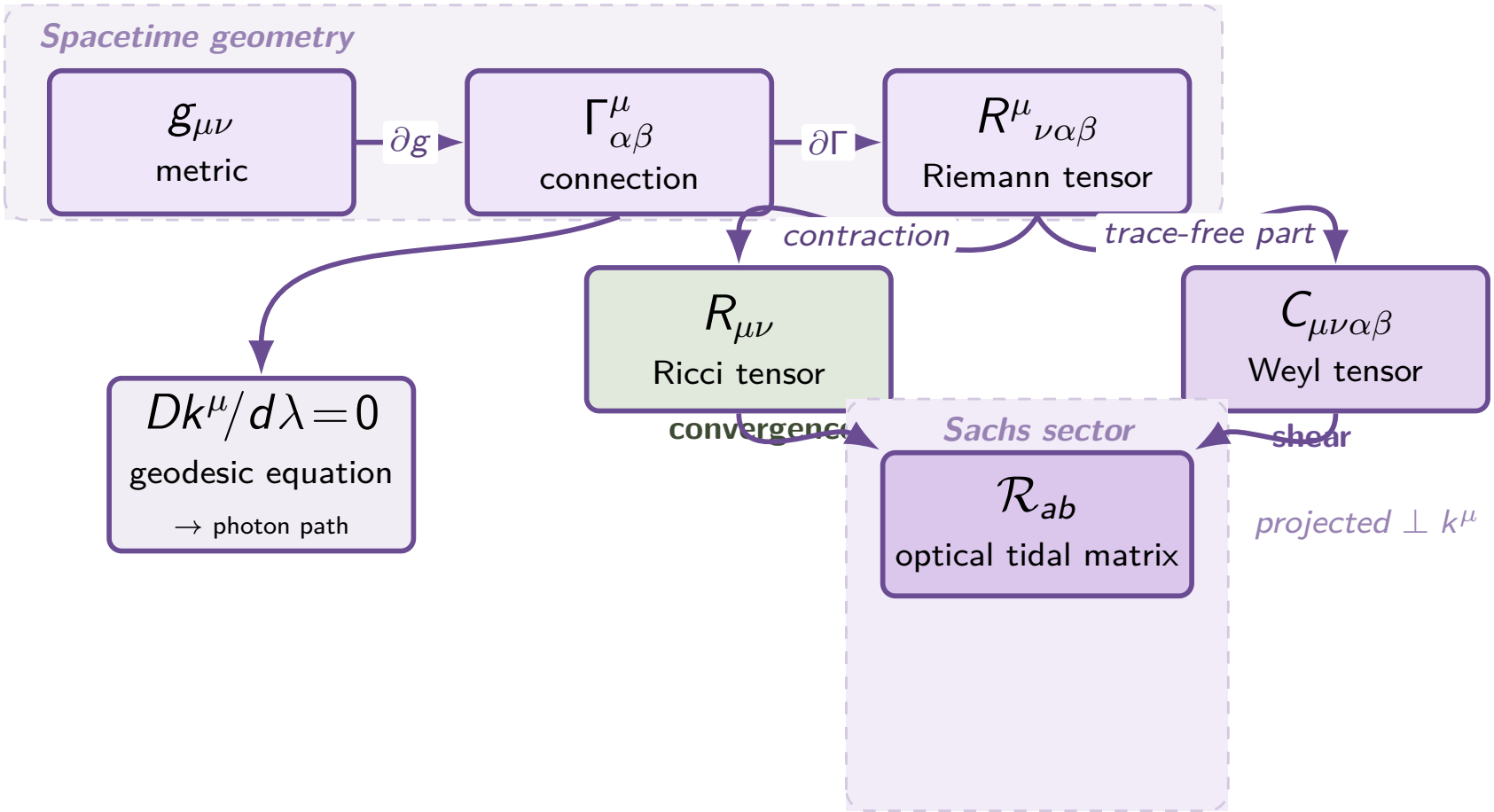
The **metric alone** fixes the whole chain: each tensor follows from derivatives of the previous one.

The tensor chain: from the metric to the Jacobi matrix



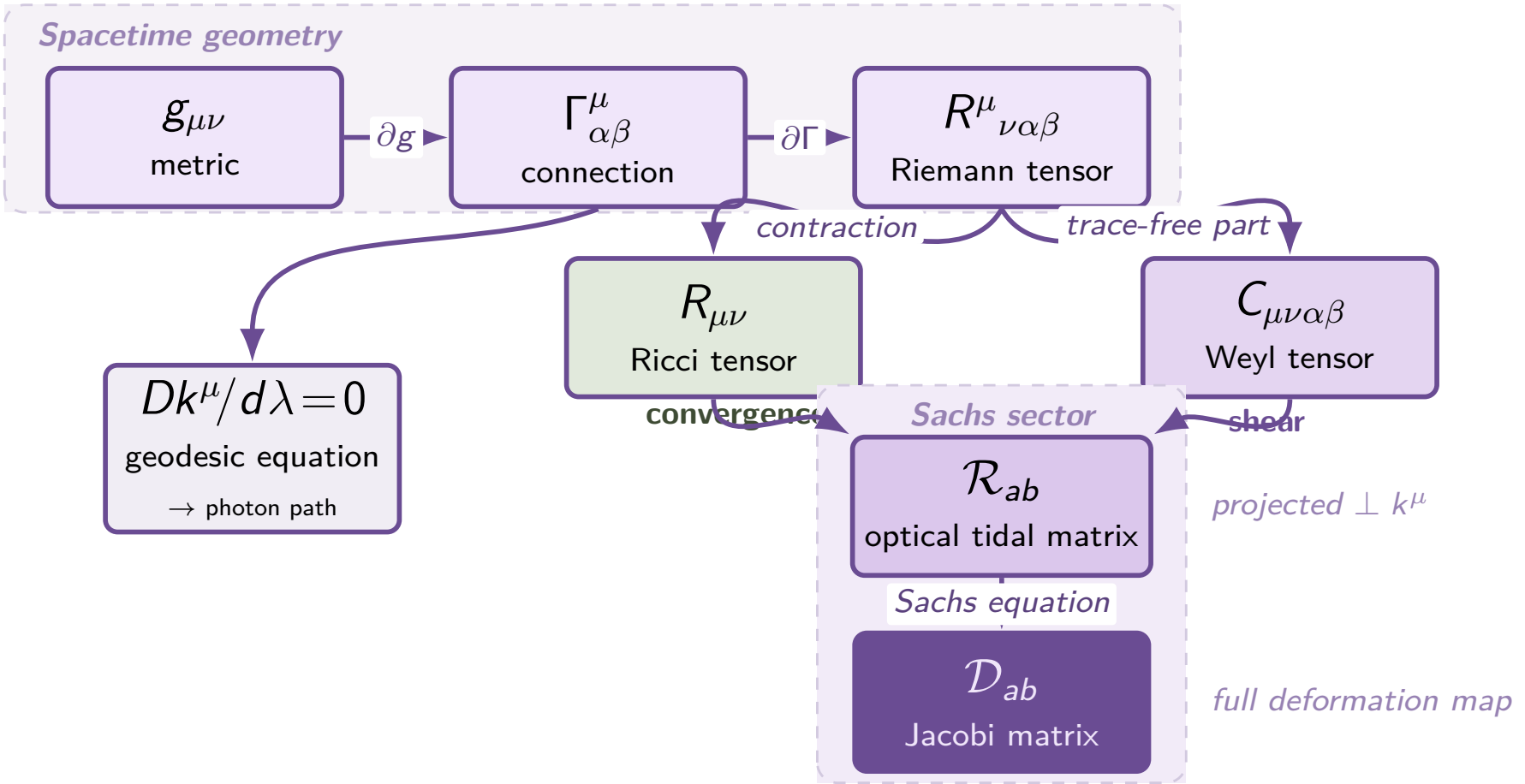
The **metric alone** fixes the whole chain: each tensor follows from derivatives of the previous one.

The tensor chain: from the metric to the Jacobi matrix



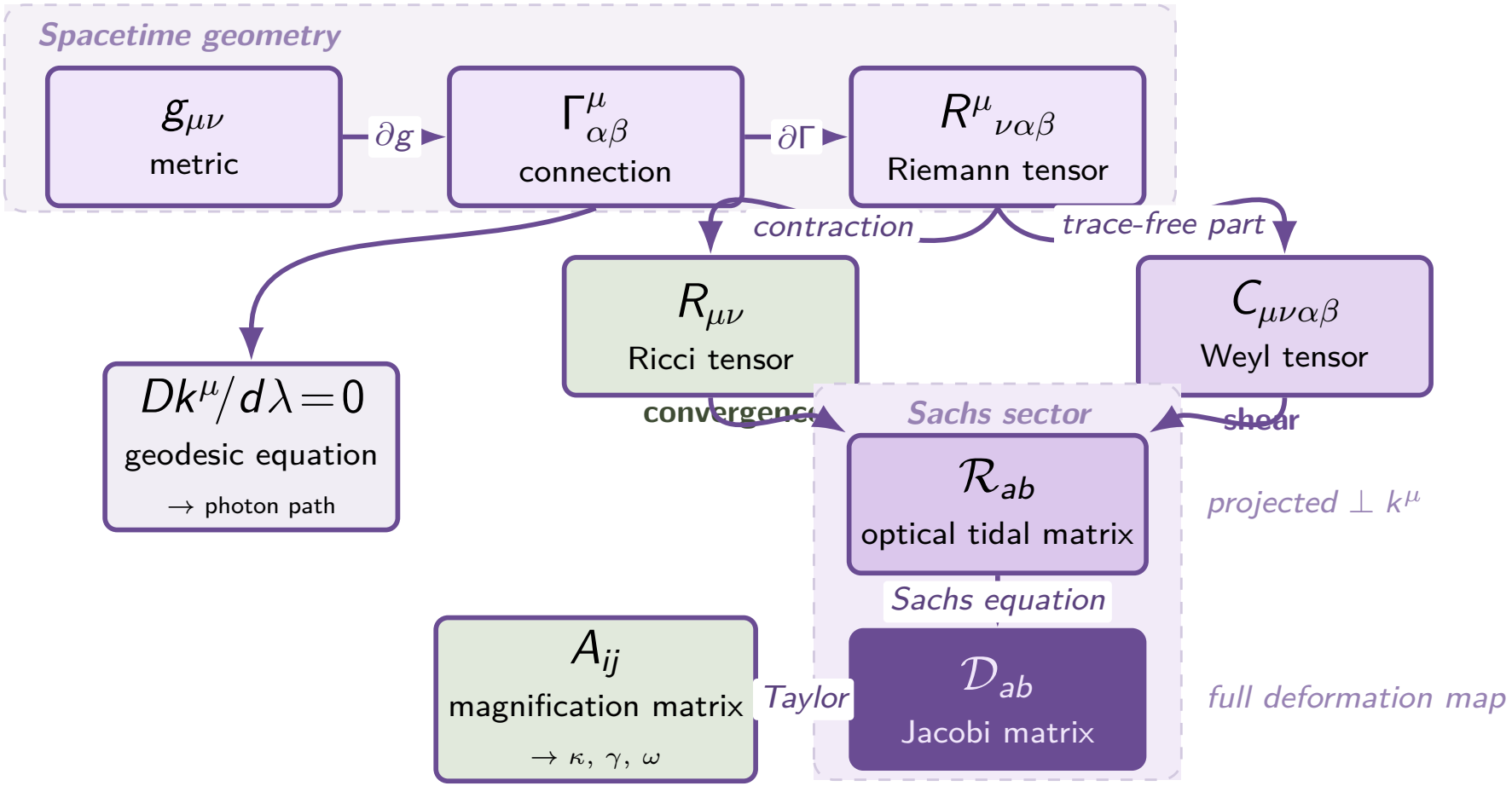
The **metric alone** fixes the whole chain: each tensor follows from derivatives of the previous one.

The tensor chain: from the metric to the Jacobi matrix



The **metric alone** fixes the whole chain: each tensor follows from derivatives of the previous one.

The tensor chain: from the metric to the Jacobi matrix



The **metric alone** fixes the whole chain: each tensor follows from derivatives of the previous one.

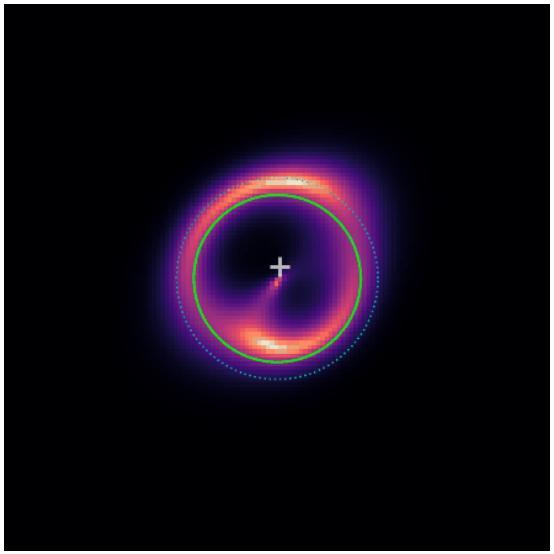
Introducing EXCALIBUR

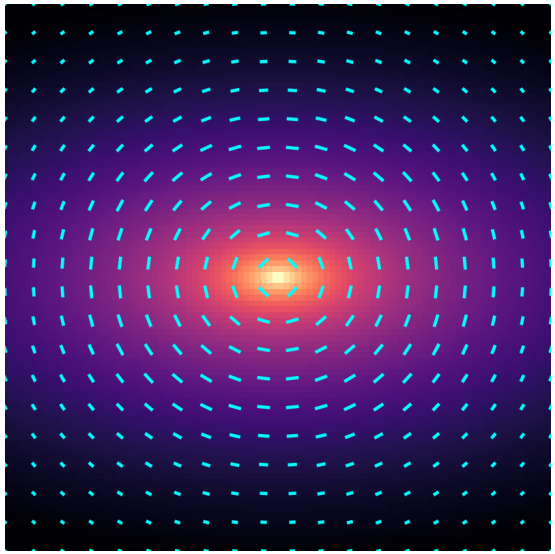
E X C A L I B U R

EX	**EX**plicit
CA	**CA**lculation (of)
LI	**LI**ght
B	**B**eams
U	**U**sing
R	**R**elativity

EXCALIBUR aims to be a modular and performant tool to compute light propagation in curved space-times.

What EXCALIBUR enables

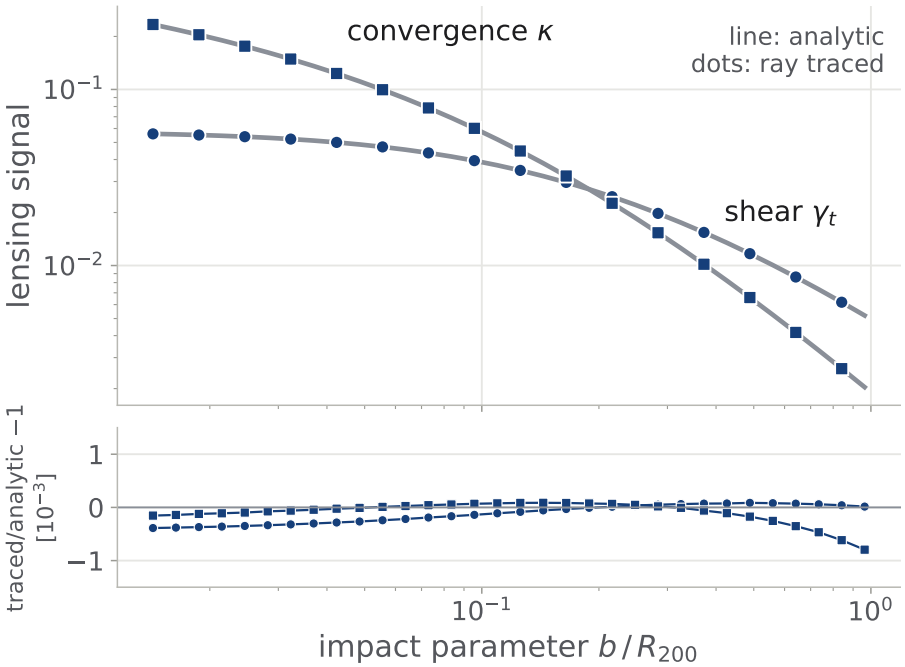




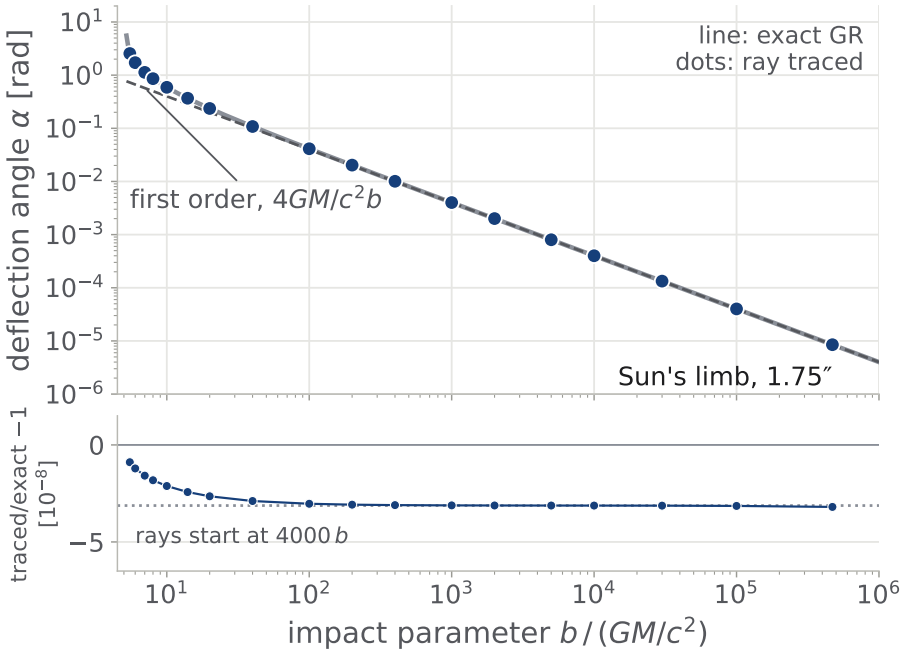
`lmagristella.github.io/assets/excalibur_lensing_webapp/`

The EXCALIBUR demo webapp

Code validation

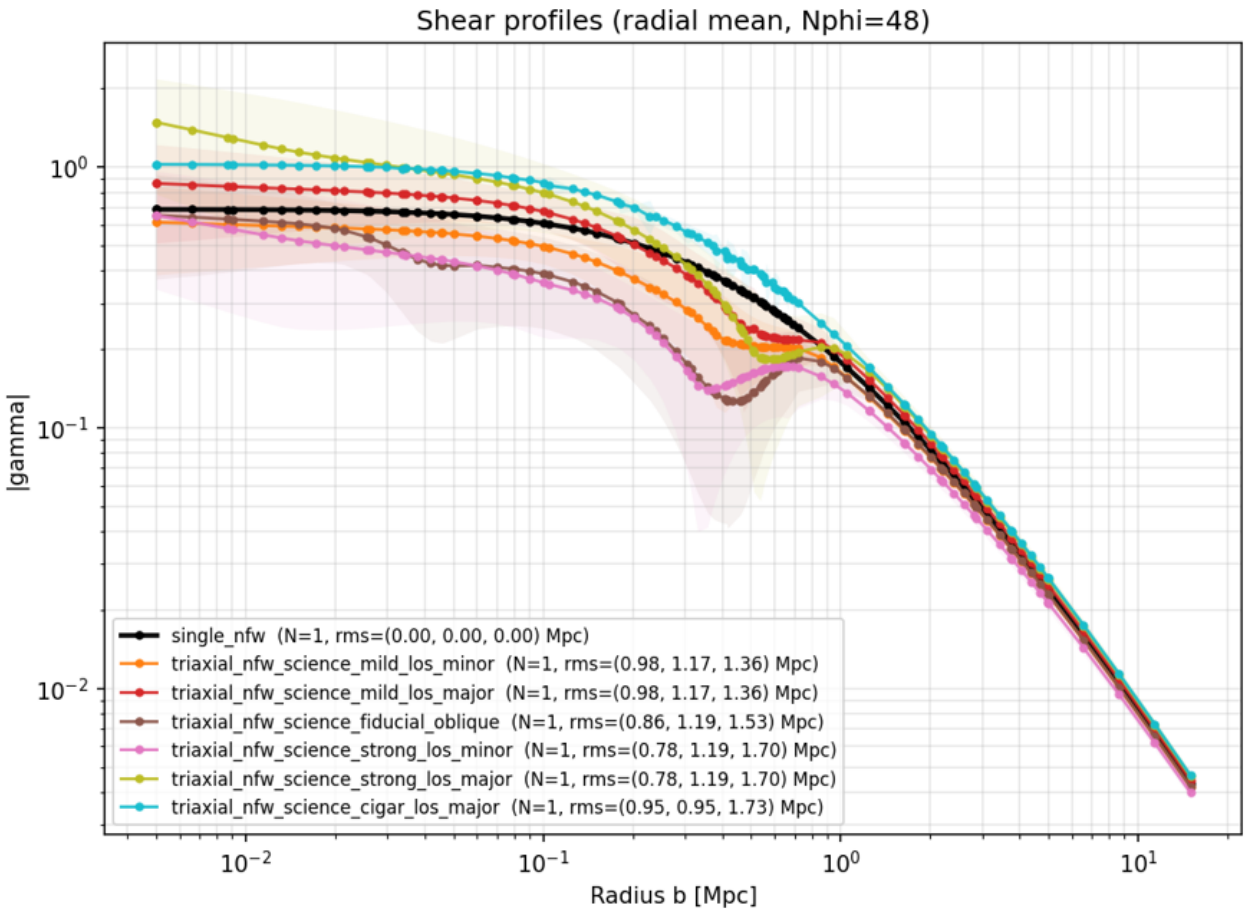


Spherical NFW halo: ray-traced κ and γ_t against the analytic profiles. They agree to $< 10^{-3}$ out to R_{200}.



Schwarzschild: ray-traced deflection angle against exact GR. They agree to 3×10^{-8}, from the Sun's limb to the strong-field regime.

Current work: model errors on mass and shape



Spherical $a=b=c$

$c\|$LOS, low e $a\approx b>c$

$c\|$LOS, high e $a\gg b>c$

$a\|$LOS, low e $a>b\approx c$

$a\|$LOS, high e $a>b\gg c$

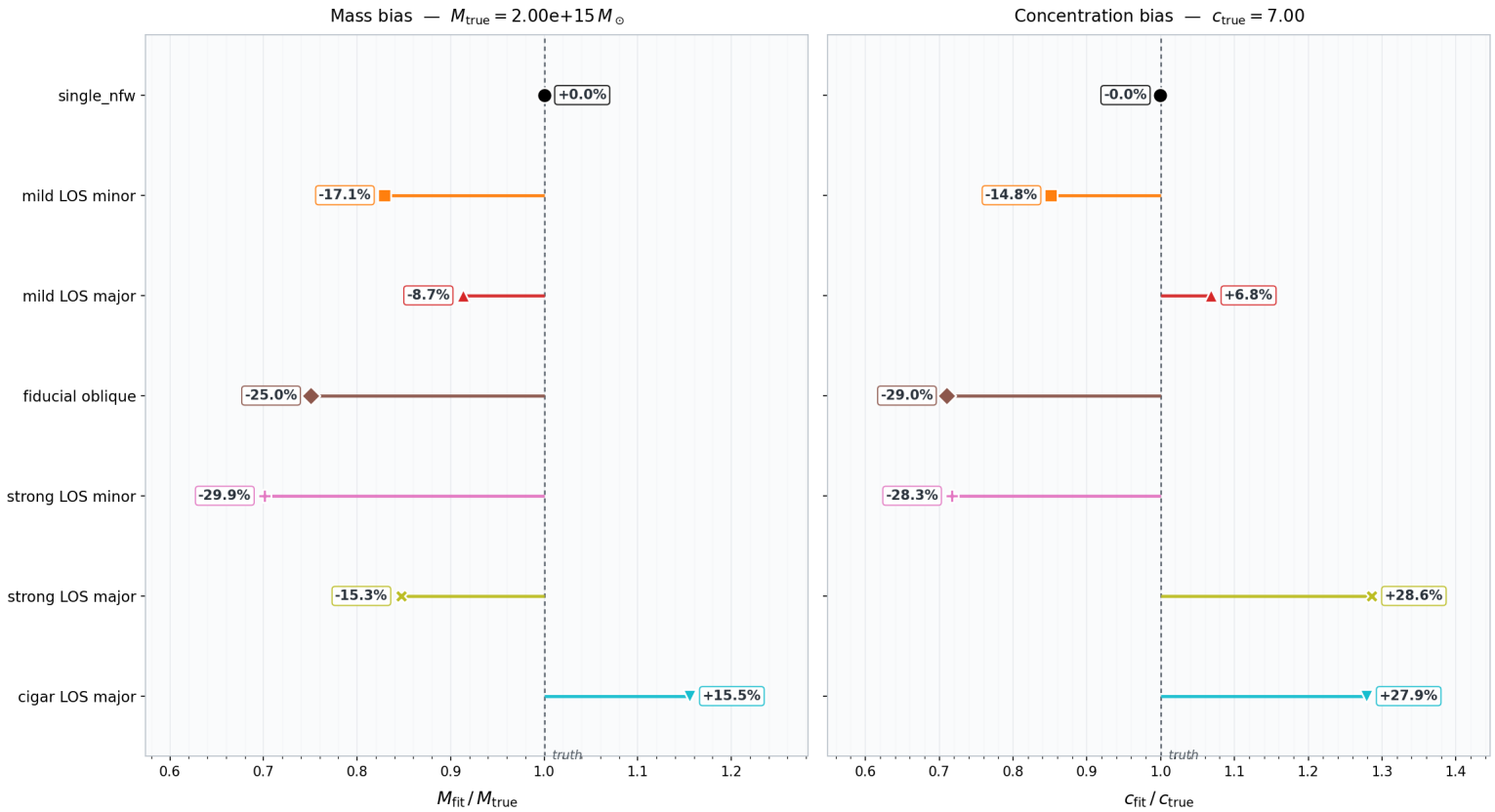
Prolate, $a\|$LOS $a\gg b=c$

Misaligned $a\neq b\neq c$

Sky-plane projections ($\perp$ LOS)

γ fit biases

Bias on inferred parameters when fitting a spherical NFW to non-spherical profiles



Spherical $a=b=c$

$c\|$LOS, low e $a\approx b>c$

$c\|$LOS, high e $a\gg b>c$

$a\|$LOS, low e $a>b\approx c$

$a\|$LOS, high e $a>b\gg c$

Prolate, $a\|$LOS $a\gg b=c$

Misaligned $a\neq b\neq c$

Sky-plane projections ($\perp$ LOS)

The simulation campaign

3 **density profiles**
NFW, Einasto, cuspy

×

4 **masses**
10^{13} to $10^{16}\ M_\odot$

×

4 **lens redshifts**
0.1 to 2,
source at $z_l + 1$

×

4 **cosmologies**
Planck, DESI,
$\Omega_m = 0.2, 0.4$

5 **concentrations**
$c = 4$ to 8

×

16 **shapes**
$q_2, q_3 \in \{0.25, 0.5, 0.75, 1\}$

×

32 **orientations**
uniformly sampled on the sphere

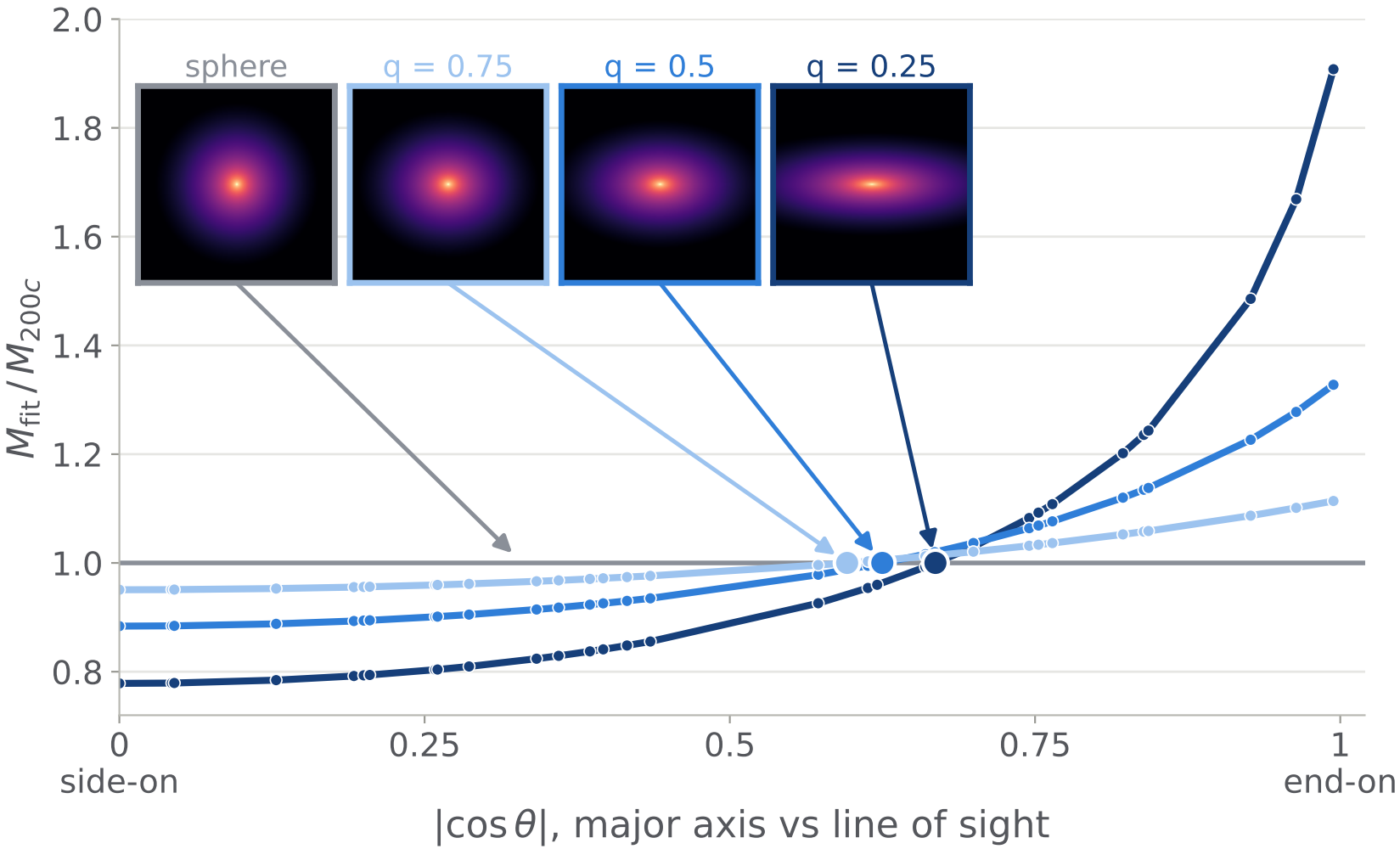
×

512^2 **rays per map**
$\kappa, \gamma_1, \gamma_2$ at each pixel

491 520 maps = 1.3×10^{11} relativistic rays

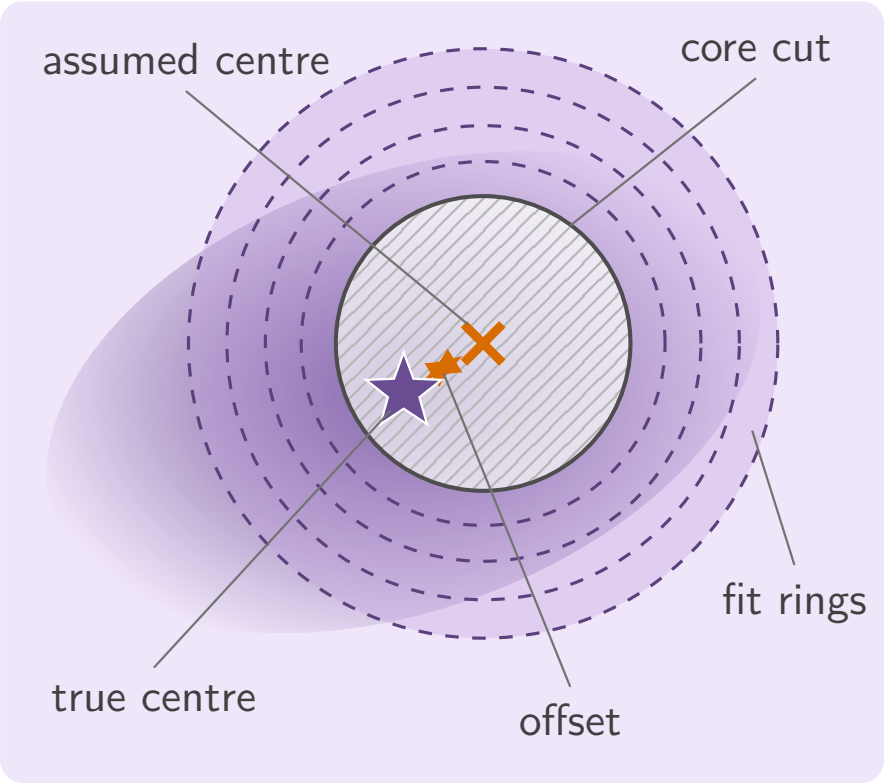
geodesic + Sachs along each ray, no Born or thin-lens approximation

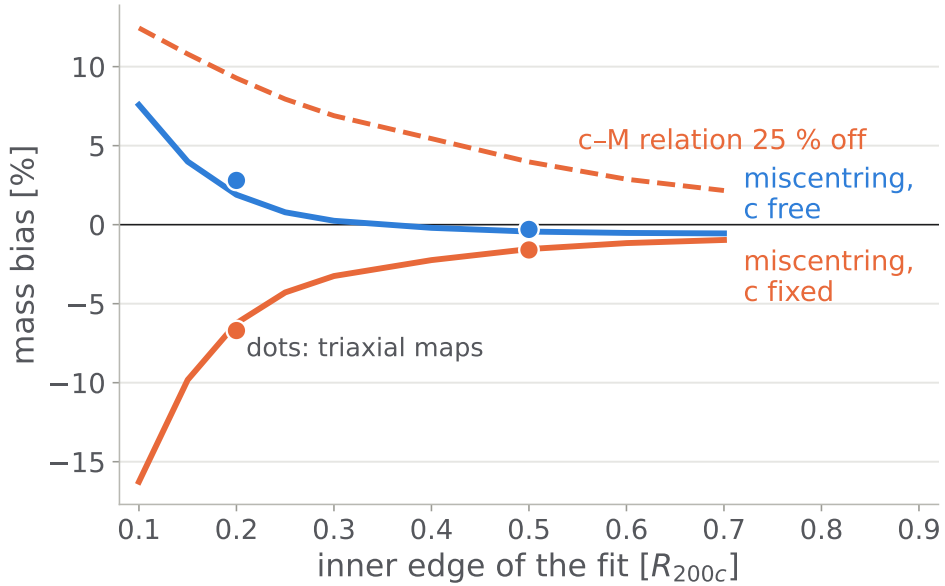
Halo mass extraction depends on its orientation

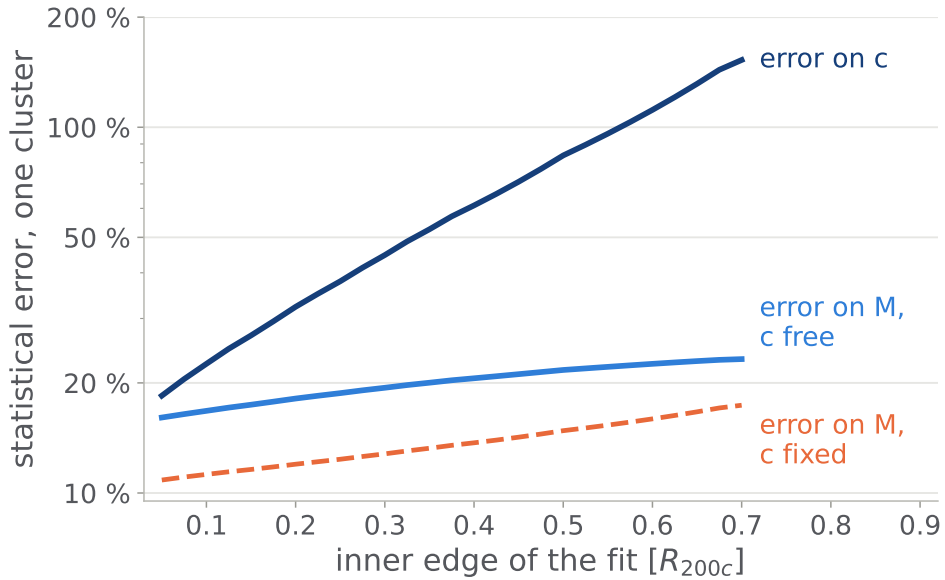


Spherical NFW fit of the reduced shear, 0.2–1.5 R_{200c}, c free. Each point: one viewing direction, median over the grid. Panels: traced κ of one halo at the crossing angle, where its own fitted mass is within 0.3% of M_{200c}; same M_{200c}, $\pm 1.5\,R_{200c}$.

The core: systematics and information

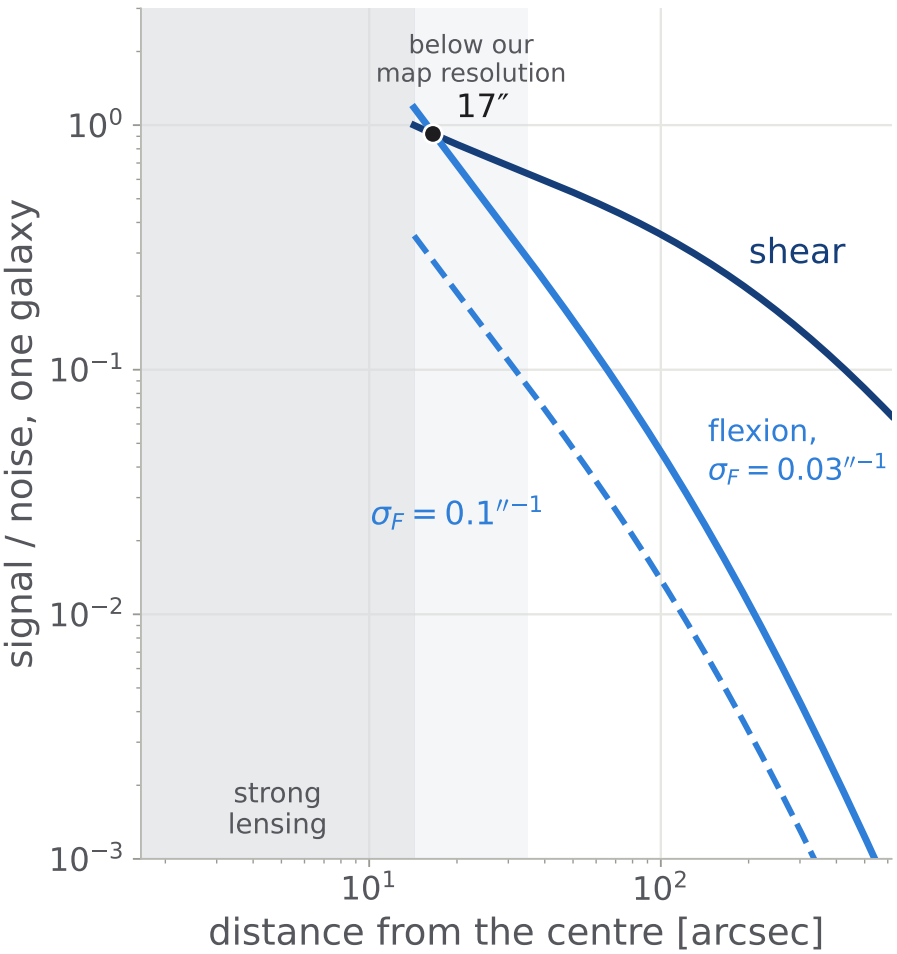


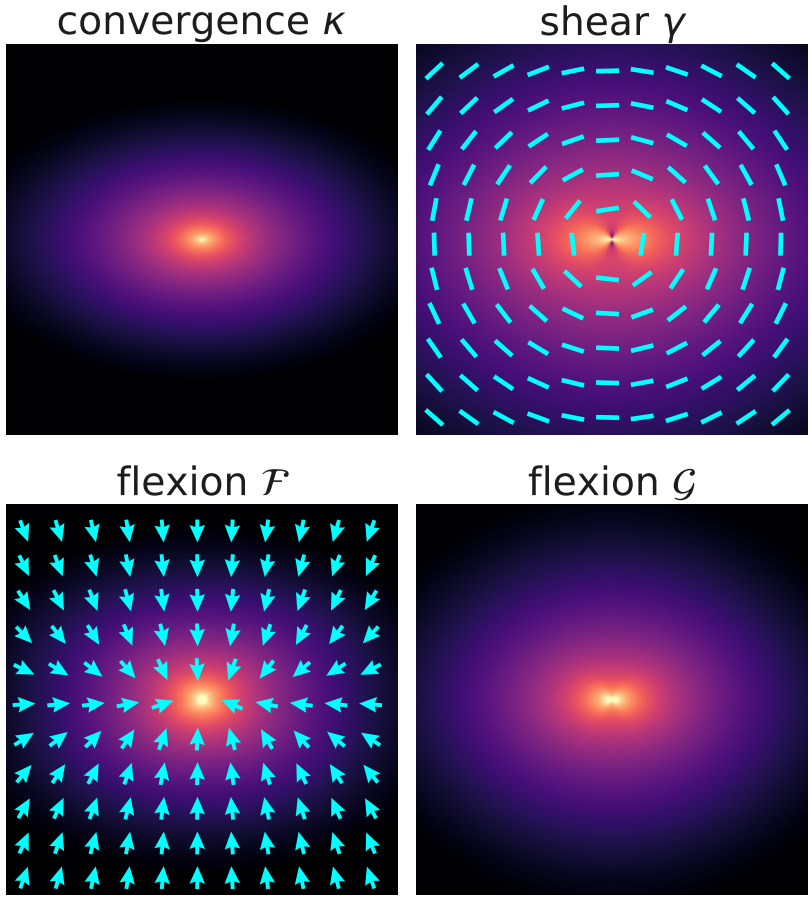




The core carries the systematics (miscentring, an imposed c) *and* the information on the concentration.

Probing the core with higher-order lensing: flexion





Flexion $\mathcal{F} = \nabla\kappa$, $\mathcal{G} = \nabla\gamma$: the lensing field of the core

A local gradient pointing at the mass peak: a handle on the centre?

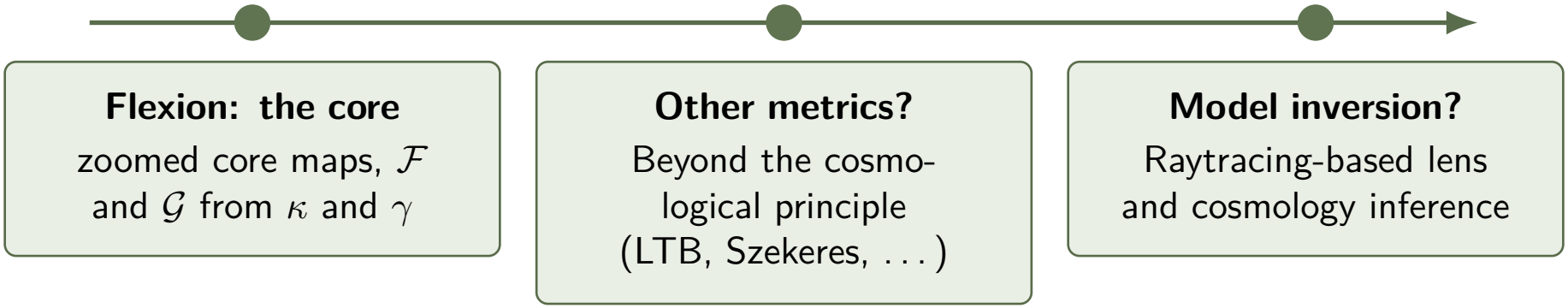
Consistent with the literature

	this work	published	references
End-on too heavy, side-on too light	**+50%, −39%**	+45%, −45%	**Corless & King 2007** **Becker & Kravtsov 2011**
Averaged over orientations, most of it cancels	**−0.8%**	mean ≈ true mass	**Corless & King 2007** **Becker & Kravtsov 2011**
With *c* fixed, the orientation leaks into *M*	**10% → 16%**	*c* free: dominates the scatter of *c*	**Bahé+ 2012** **Oguri & Blandford 2009**
Selection favours end-on halos, masses too high	**+1.5 to +2.3%**	up to +3–6%	**Dietrich+ 2014** **Zhang+ 2023**
Random SZ offsets lower *M* at fixed *c*	**−2.2%**	−3.1%	**Sommer+ 2024**
Cutting the core lowers the mass systematics	**miscentring ÷ 4**	uncertainty ÷ 1.2–1.5	**Grandis+ 2021** **Sommer+ 2022**
A wrong *c*–*M* relation moves the mass	**+4 to +10%**	mean bias 0.9 to 1.1	**Sommer+ 2022**

This work uses isolated halos; the published values come from other simulations and set-ups.

Conclusion and outlook

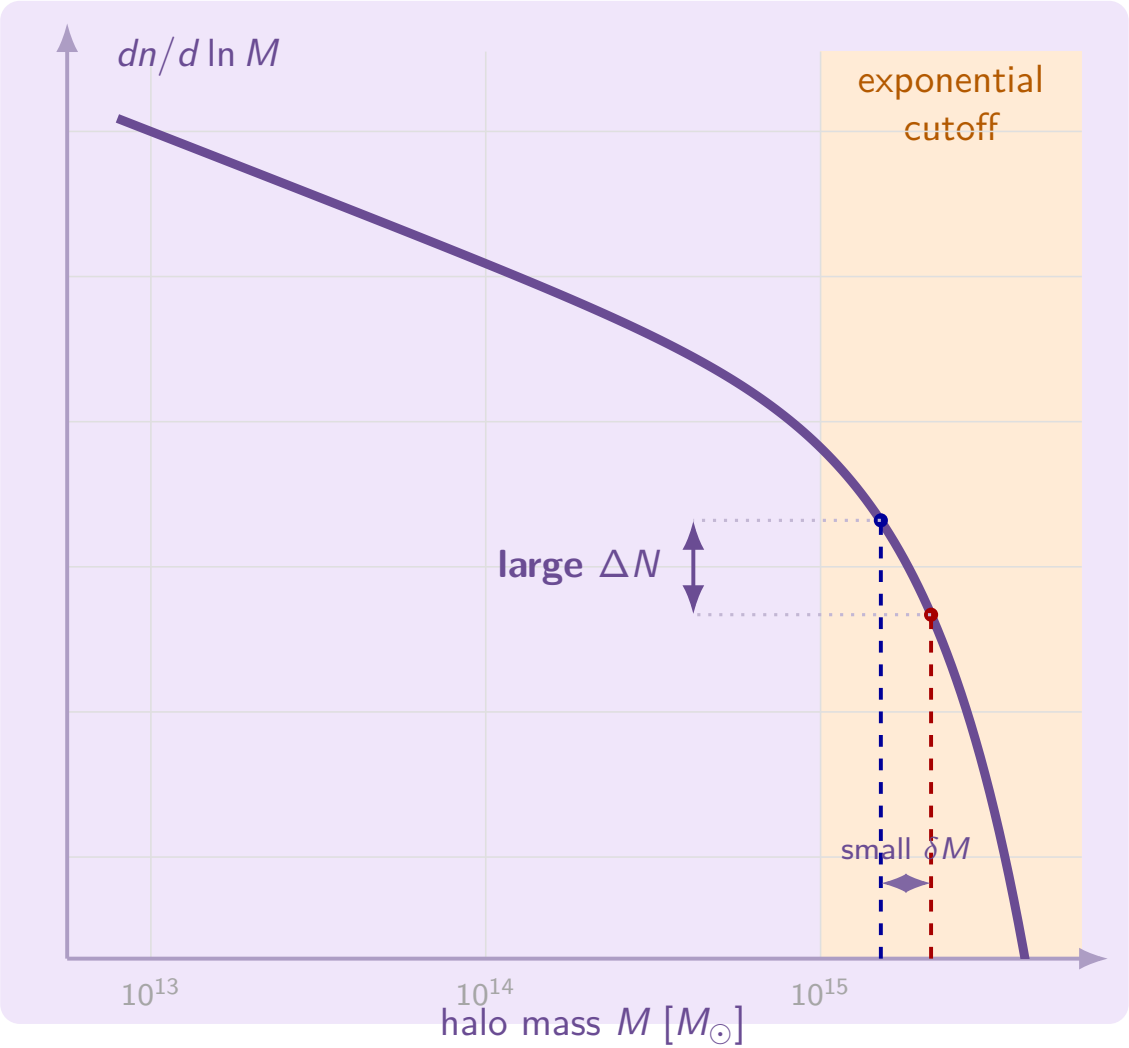
Perspectives



Take home message

excalibur: a modular relativistic raytracing code, validated against test cases. Triaxiality spreads the mass of one cluster by $\pm 10\%$; selection and analysis choices (c, inner cut) turn it into biases up to $\sim 10\%$.

The halo mass function amplifies mass biases



Halo mass function

$dn/d\ln M$: comoving number density of halos per unit mass.

Steep cluster-scale tail

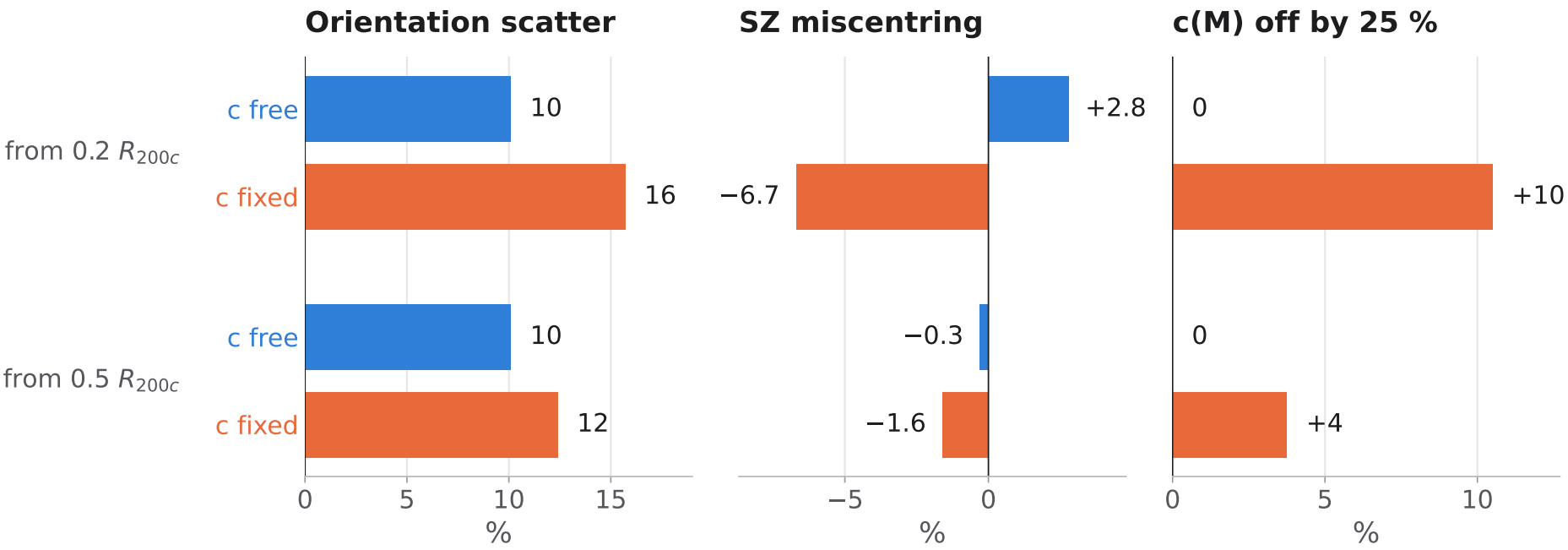
At high mass it falls exponentially

$$\frac{dn}{d\ln M} \propto e^{-\delta_c^2/2\sigma^2(M)}$$

Why it matters

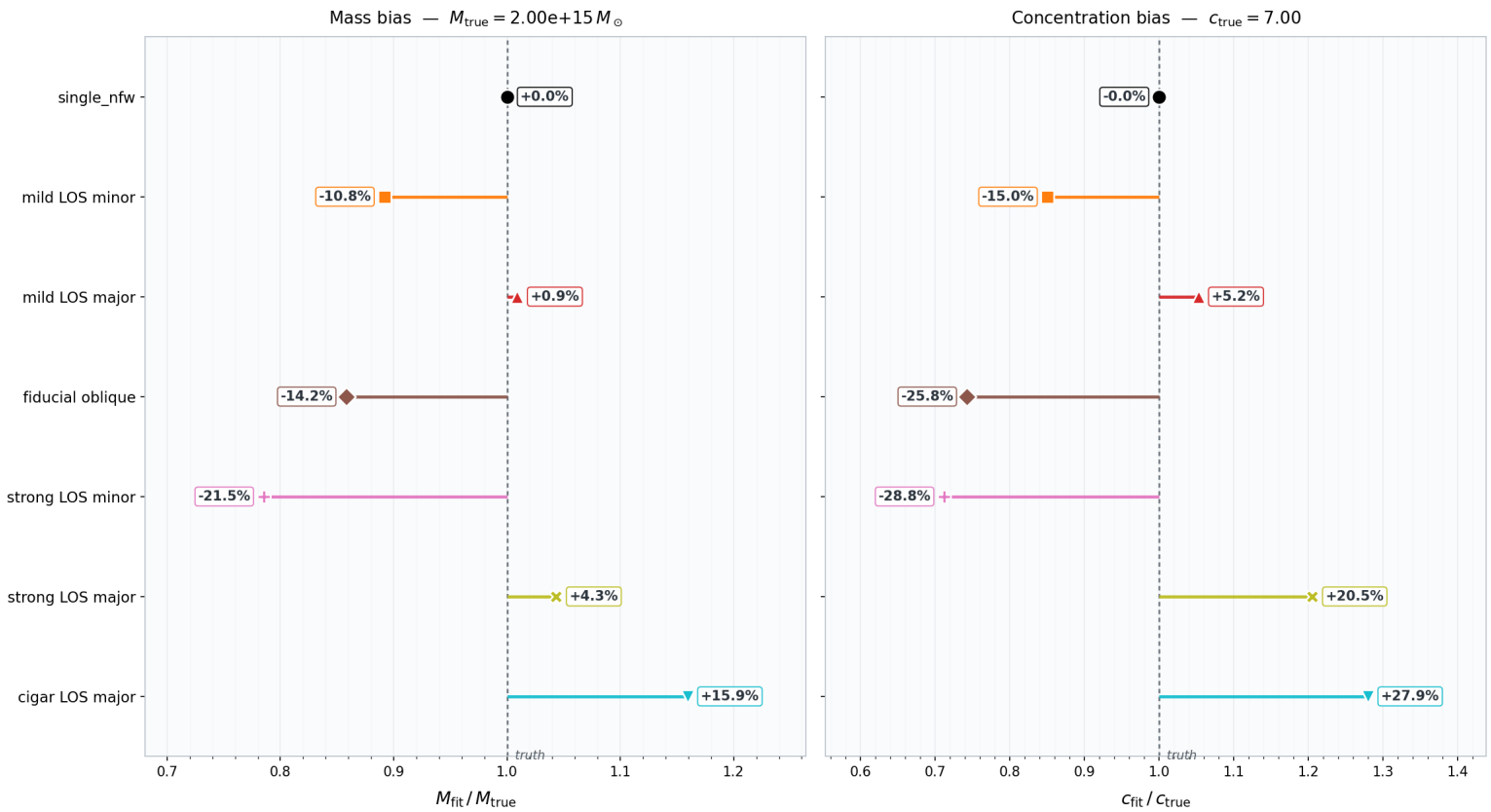
A few-% bias on $M \Rightarrow$ **large** bias on cluster counts $\Rightarrow$ biased cosmology (σ_8, Ω_m).

Fit c or impose it? Keep the core or cut it?



- Fixing c, even at its true value, leaks the orientation into M (10% $\rightarrow$ 16%).
- Miscentring changes sign with the treatment of c.
- Fitting from $0.5\,R_{200c}$ shrinks every systematic, for +20–30% of statistical error.

Appendix: Joint κ, γ fit biases



Spherical $a=b=c$

$c \| $ LOS, low e $a \approx b > c$

$c \| $ LOS, high e $a \gg b > c$

$a \| $ LOS, low e $a > b \approx c$

$a \| $ LOS, high e $a > b \gg c$

Prolate, $a \| $ LOS $a \gg b = c$

Misaligned $a \neq b \neq c$

Sky-plane projections ($\perp$ LOS)

Backup: Spherical NFW profile

3D density (Navarro, Frenk & White 1997)

$$\rho(r) = \frac{\rho_s}{\frac{r}{r_s}\left(1+\frac{r}{r_s}\right)^2}$$

- ρ_s: characteristic density
- $r_s = R_{\rm vir}/c$, concentration c
- slope -1 for $r \ll r_s$; slope -3 for $r \gg r_s$

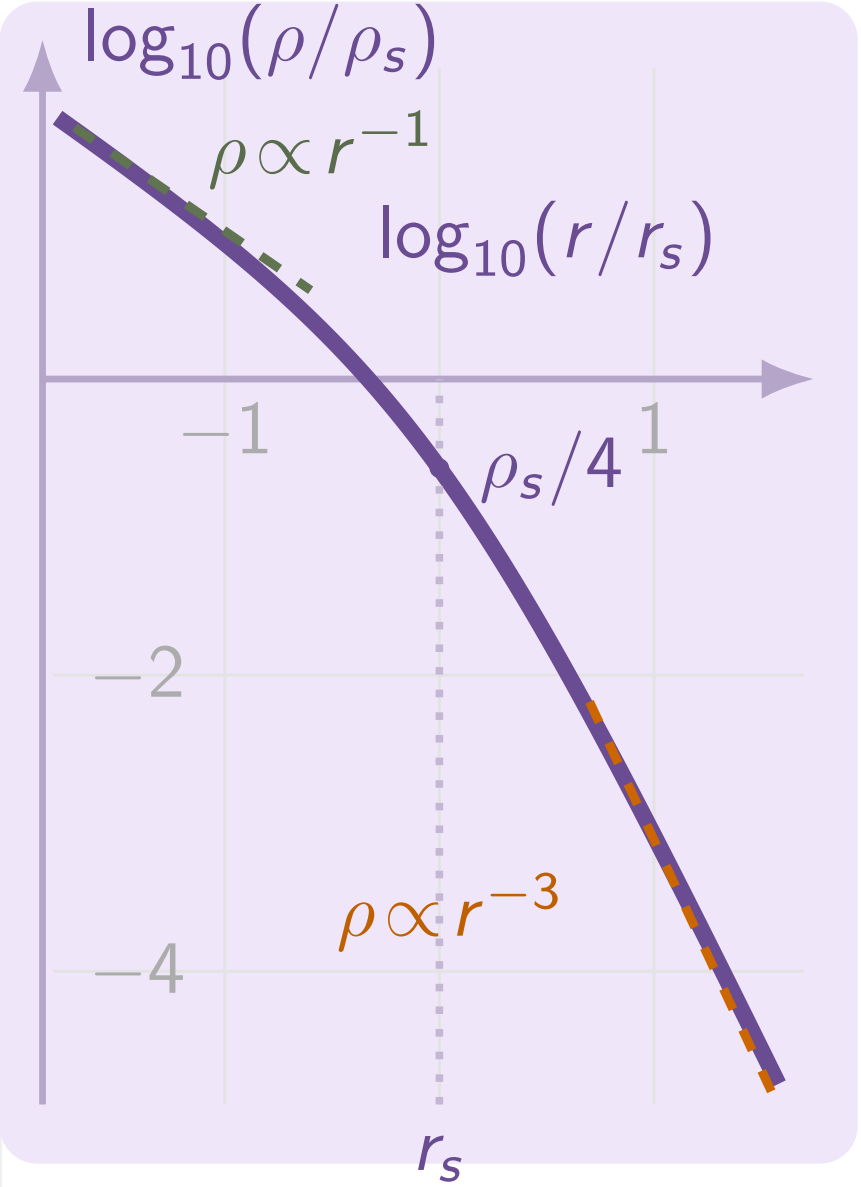
Projected convergence

$$\kappa(\xi) = \frac{2}{\Sigma_{\rm cr}} \int_0^\infty \rho\left(\sqrt{\xi^2+z^2}\right) dz$$

Analytic form: Wright & Brainerd (2000)

Role in this work

Reference (symmetric) case used to quantify triaxiality-induced biases.



Backup: Triaxial NFW profile

Triaxial generalization (Jing & Suto 2002)

Replace r by $m = \sqrt{x^2/a^2 + y^2/b^2 + z^2/c^2}$ ($a \geq b \geq c$):

$$\rho_{\rm triax}(\mathbf{x}) = \rho_{\rm NFW}(m)$$

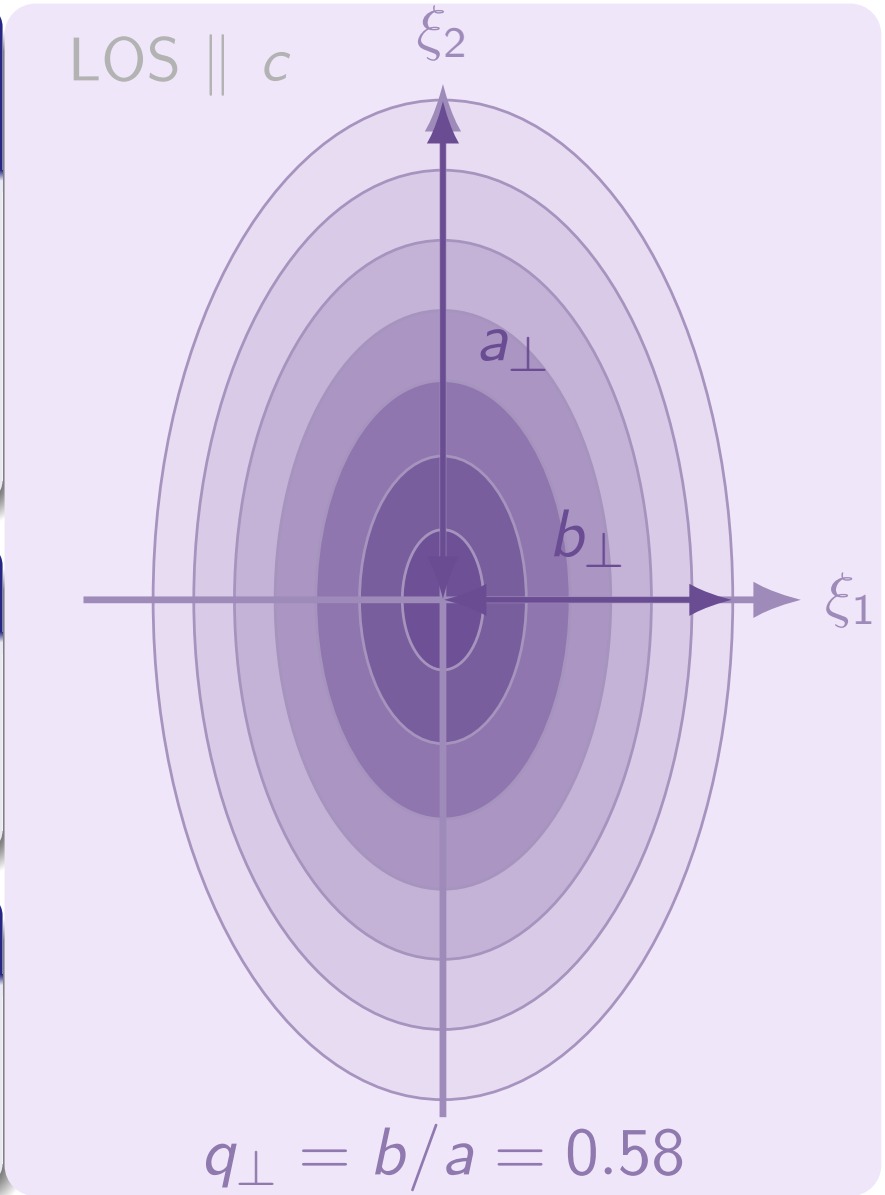
Projected convergence (LOS $\parallel$ c)

$$\kappa(\xi_1, \xi_2) \propto \int_{-\infty}^{+\infty} \rho_{\rm NFW}(m)\, dz$$

$\rightarrow$ **Elliptical** contours, $q_\perp = b/a$.

Consequence

Fitting a spherical model to a triaxial halo biases the inferred mass and concentration (Corless & King 2007).



Backup: Schwarzschild deflection angle

Exact result, with $m = GM/c^2$ and $u = 1/r$

$$\alpha(b) = 2\int_0^{u_0} \frac{du}{\sqrt{1/b^2 - u^2 + 2m\,u^3}} \;-\; \pi$$

u_0: closest approach. α diverges at the photon sphere, $b_c = 3\sqrt{3}\,m$.

Expansion in $\varepsilon = m/b$

$$\alpha = \underbrace{4\,\varepsilon}_{\text{Einstein}} + \frac{15\pi}{4}\,\varepsilon^2 + \frac{128}{3}\,\varepsilon^3 + \frac{3465\pi}{64}\,\varepsilon^4 + \ldots$$

series up to	$b = 10\,m$	$b = 20\,m$	$b = 100\,m$	Sun's limb
ε^1	32%	15%	3%	6×10^{-4} %
ε^2	12%	2.8%	0.11%	5×10^{-9} %
ε^3	5.1%	0.57%	4×10^{-3} %	4×10^{-14} %
ε^4	2.2%	0.12%	2×10^{-4} %	4×10^{-19} %

Shortfall of the truncated series. Darwin (1959); Keeton & Petters (2005).

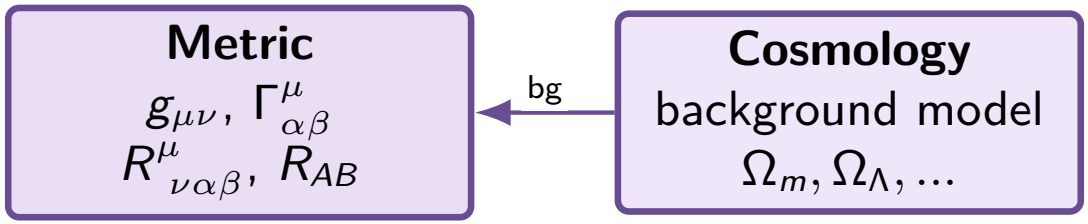
EXCALIBUR: numerical pipeline

Metric

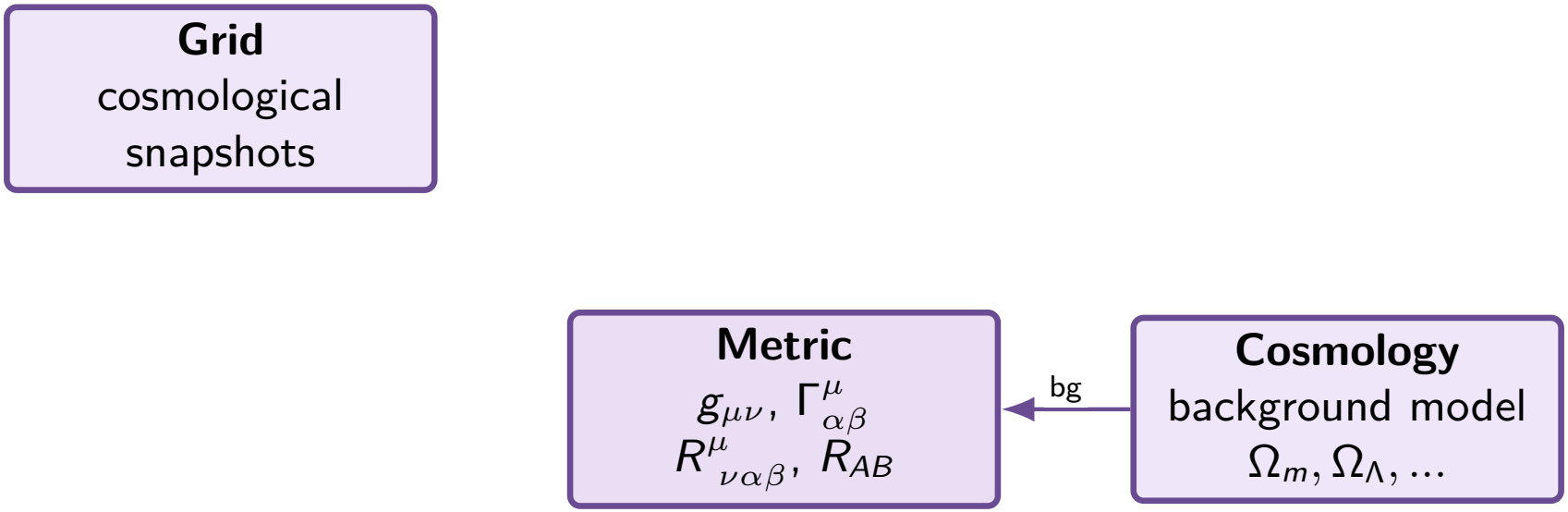
$g_{\mu\nu}$, $\Gamma^{\mu}_{\alpha\beta}$

$R^{\mu}_{\nu\alpha\beta}$, R_{AB}

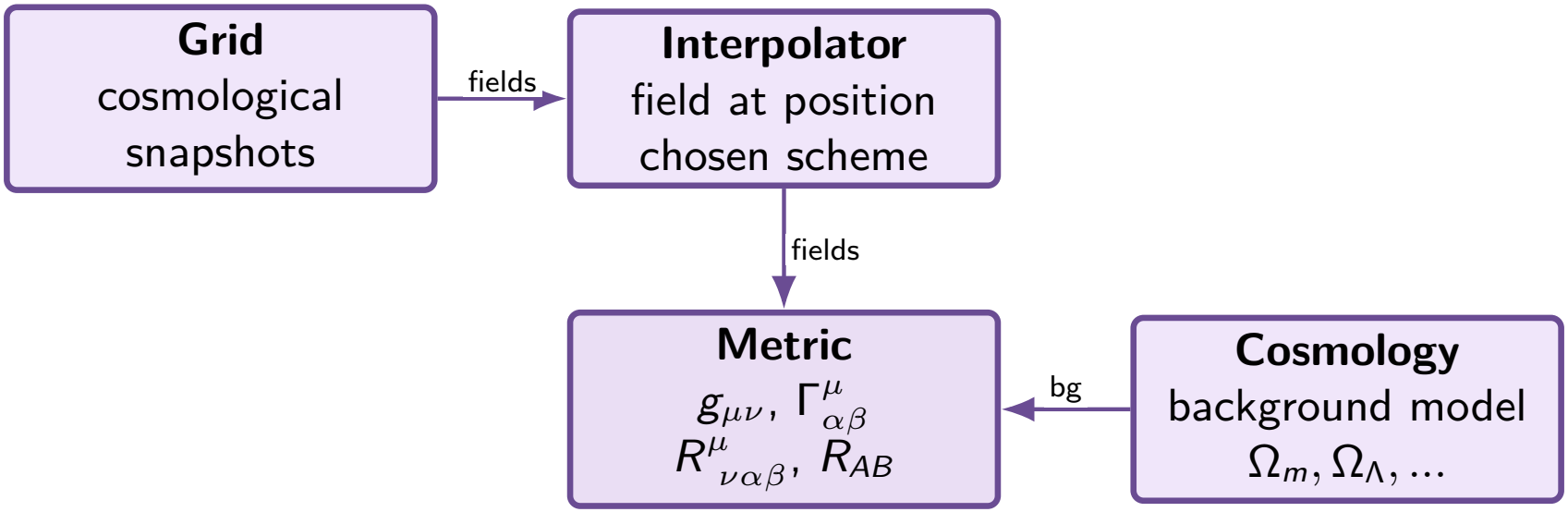
EXCALIBUR: numerical pipeline



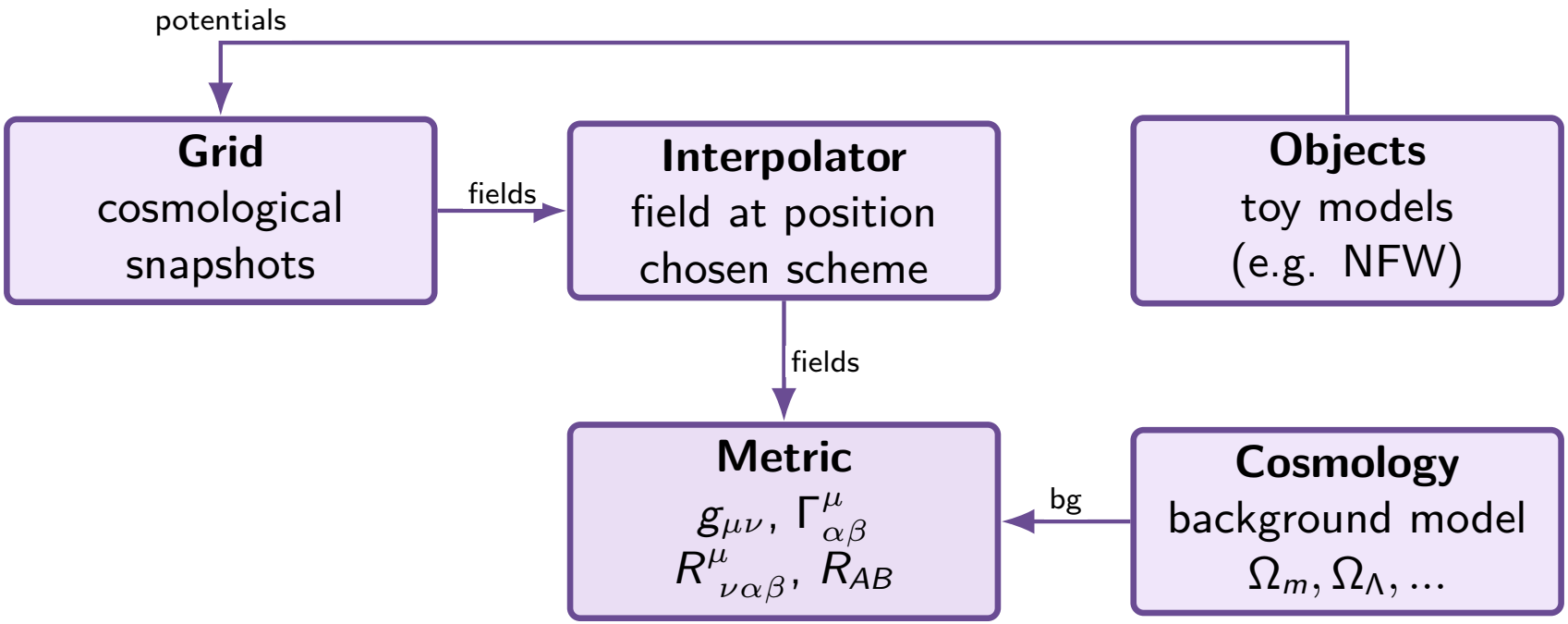
EXCALIBUR: numerical pipeline



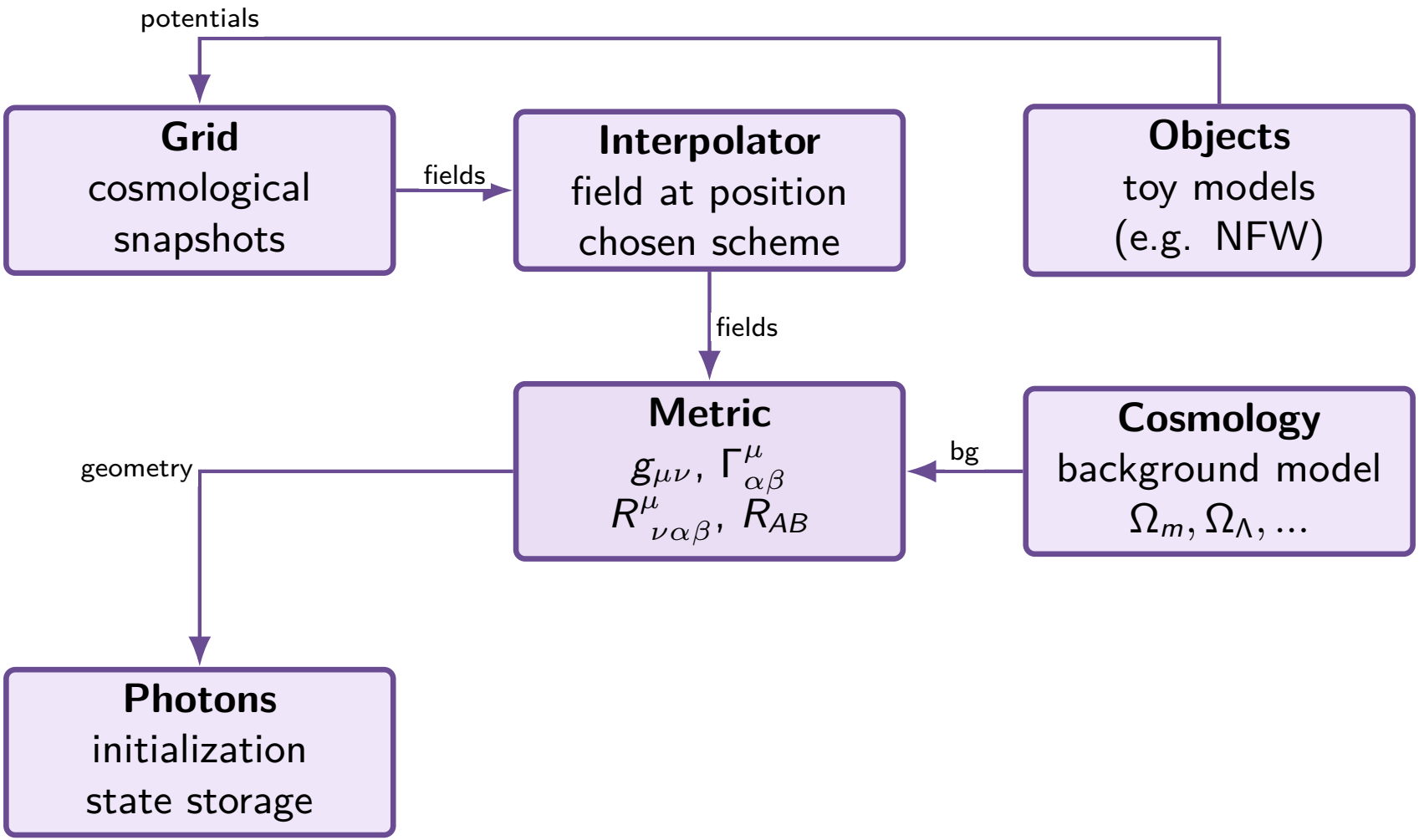
EXCALIBUR: numerical pipeline



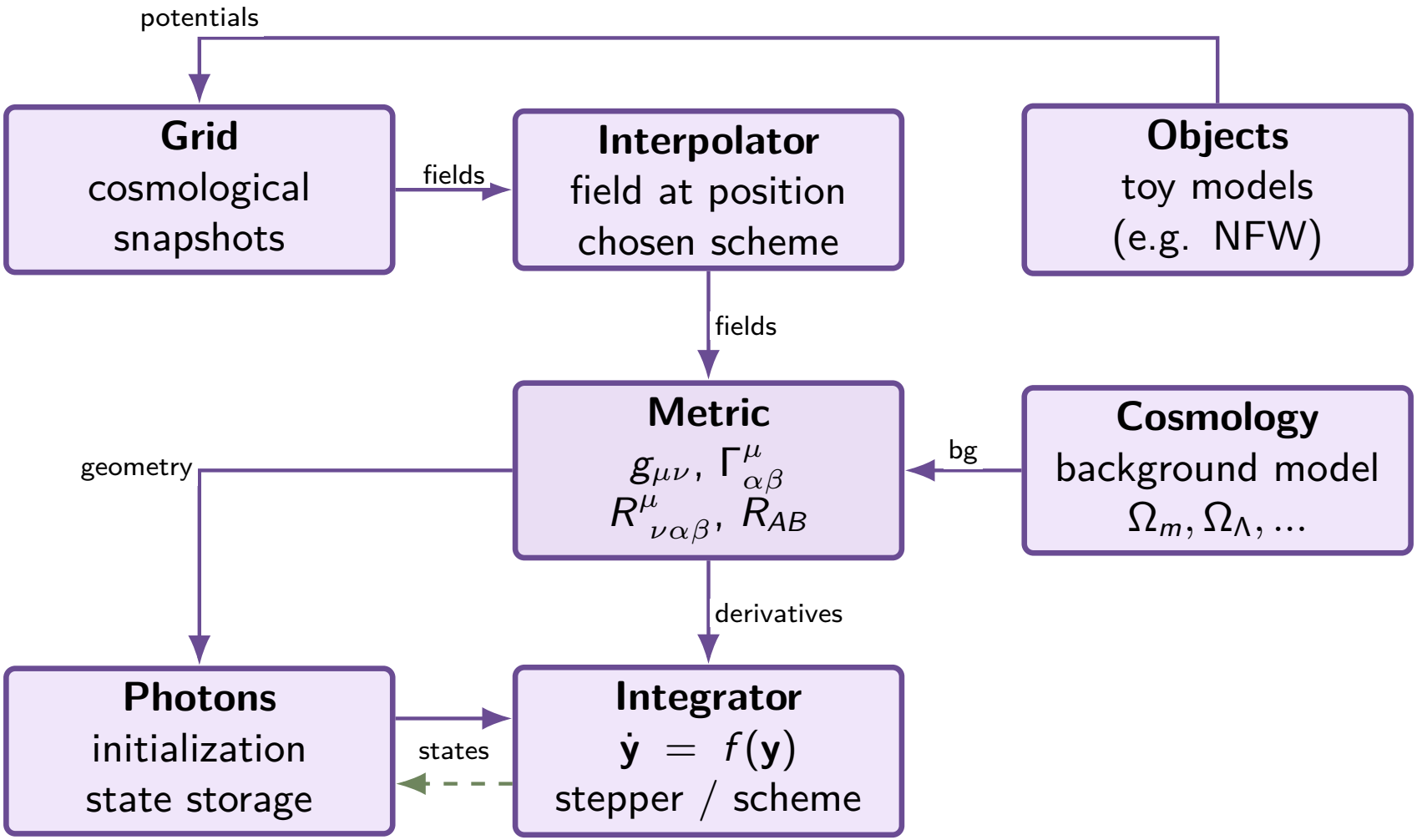
EXCALIBUR: numerical pipeline



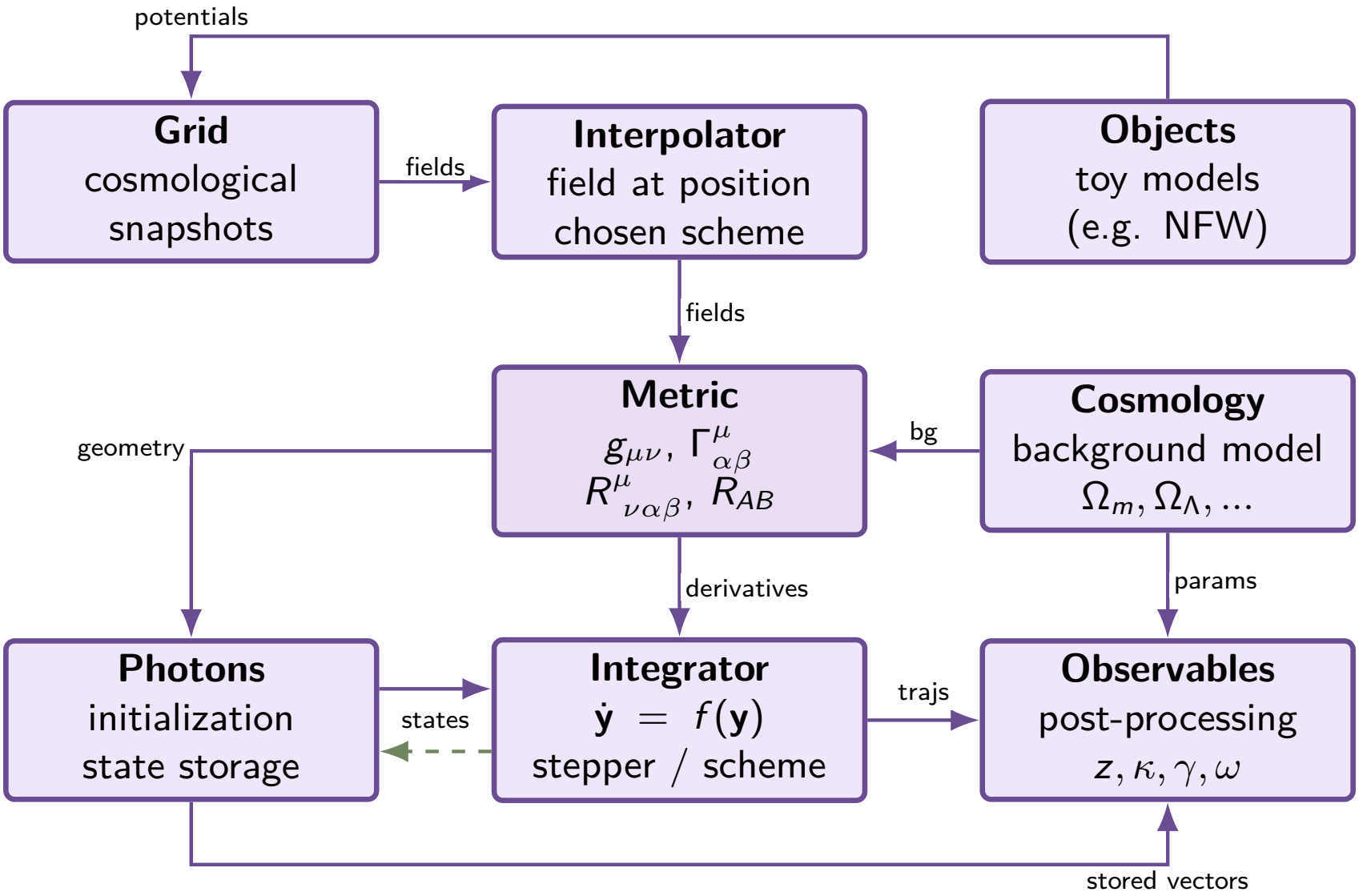
EXCALIBUR: numerical pipeline



EXCALIBUR: numerical pipeline



EXCALIBUR: numerical pipeline



Already existing raytracing codes?

Code name	References	Metric	Input	Applications
GEVOLUTION RAYTRACER	J. Adamek 2018	weak-field	gevolution simulations	cosmology, relativistic light cones, redshifts, distances
MAGRATHEA	V. Reverdy 2014, M.A. Breton and V. Reverdy 2021	weak-field	large-scale cosmological simulations	cosmology, relativistic light cones, redshifts, distances, large-scale structures
GYOTO	F. H. Vincent 2011	analytic, 3+1 full GR	analytic models or LORENE code	compact objects
EXCALIBUR	**L. Magri-Stella, V. Reverdy, N. Lorenzo-Martinez 2026**	**analytic, weak-field**	**analytic models or large-scale structure**	**cosmology, large-scale structures, gravitational lensing**

A gap to fill?

No existing code simultaneously targets weak-field cosmology, large-scale structure, and gravitational lensing in a relativistic framework.